CNN and Ensemble Learning for Brain Tumor Segmentation and Survival Prediction

By

Ali Nawaz

00000319412

Supervisor

Dr. Muhammad Usman Akram

Department of Computer Software Engineering

College of Electrical and Mechanical Engineering

National University of Sciences and Technology (NUST)

Islamabad, Pakistan

July 2021

CNN and Ensemble Learning for Brain Tumor Segmentation and Survival Prediction

By

Ali Nawaz

00000319412

Supervisor

Dr. Muhammad Usman Akram

A thesis submitted in conformity with the requirements for

the degree of *Master of Science* in

Software Engineering

Department of Computer & Software Engineering

College of Electrical Mechanical Engineering

National University of Sciences and Technology (NUST)

Islamabad, Pakistan

July 2021

Declaration

I, *Ali Nawaz* declare that this thesis titled "CNN and Ensemble Learning for Brain Tumor Segmentation and Survival Prediction" and the work presented in it are my own and has been generated by me as a result of my own original research.

_____

Ali Nawaz,

00000319412

Copyright Notice

This thesis is dedicated to *my beloved parents*

Abstract

Brain tumor is the spread of abnormal cells in the brain. Out of several kinds of brain tumor gliomas is the most dangerous with low survival rate and difficult to detect manually due to irregular form and confusing boundaries. Magnetic Resonance Imaging is the most widely used imaging modality that allows radiologist to look inside brain by utilizing radio waves and magnet but the manual identification of tumor region is tedious task. Therefore, a reliable and automatic segmentation and prediction is necessary for segmentation of brain tumor and prediction. However due to complexity and unavailability of resources to train deep learning algorithms, it is complex to identify the tumorous and non-tumorous region. So, in this paper, a reliable and efficient variant of UNET i.e., VGG19-UNET for segmentation of brain tumor and ensemble learning model for survival prediction is proposed. Specifically, an encoder part of the UNET is a pretrained VGG19 followed by the adjacent decoder part. Meanwhile, the ensemble voting classifier of Naïve Bayes and Random Forest was trained for survival prediction. The datasets we are using for segmentation is BRATS'20 which comprises of four different MRI modalities and one target mask file. Whereas, the datasets of survival prediction is also BTARS'20 which is comma separated file containing different features. Above mentioned algorithm resulted in dice coefficient score of 0.81, 0.86 and 0.88 for enhancing, core and whole tumor whereas the accuracy of overall survival is 62.7%. **Keywords:** *VGG19, UNET, Encoder-Decoder Network, Segmentation of brain tumor, MRI, Survival Prediction, Ensemble Learning, BRATS*

Acknowledgments

All praise to Allah (the omnipotent and the omnipresent) who has bestowed me with ardor, courage, and patience with which I have completed another phase of my academic journey.

I want to mention some special people who have played a pivotal role in my life and gave me enormous courage and motivation. Firstly, I would like to dedicate this MS to my parents, who have done all the hard work for me in my life. They encouraged me to continue my higher studies and full-heartedly supported my passion and my dream. Additional to this, I also want to mention my younger brother and elder sister. They believed in me and provided unwavering support throughout my journey.

And most importantly, I want to pay special gratitude to my Supervisor Dr. Usman Akram, without whom I would not have been able to take this task to fruition. He not only enlightened the path for me but also made me competent enough to hold my ground against all the odds.

In the last, I am thankful to all my friends and dear ones who stood with me against every thick and thin and motivated me throughout.

Contents

List of Figures

List of Tables

CHAPTER 1

INTRODUCTION

Brain tumor is the spread of atypical cell in the brain. Some cells are non-cancerous (benign) having high survival rate while some cells are cancerous (malignant) having low survival rate [1]. There are two kinds of brain tumors. First is known as primary tumor because it starts from brain it is the common kind of tumor and other one is known as secondary tumor because it travels from other part in the body and extends to the brain [2]. There are several types of brain tumor out of which gliomas are the most ordinary type of brain cancer and more than 35 percent of all brain cancers are gliomas. Gliomas originates from glial cells which are responsible for keeping neural nerves healthy. Gliomas is further divided into several types based on the specific targeted cell. Out of which, a glioblastoma is the most malignant type of the glioma [8].

MRI is an imaging technique that allow doctors to see inside human body by utilizing magnet and radio waves. As brain is the most common soft tissue therefore MRI provide excellent detail of the brain image as compared to CT, X-ray and Ultrasound modalities. To get better results of the targeted areas certain types MRI modalities are employed amongst them T1, T2, T2* and FLAIR weighted mages are most common modalities of MRI [3], [4]. TI weighted images are produced by using little Repetition Time (TR) and Time to Echo (TE), while T2 weighted images are produced by using greater TR and TE than T2. Similarly, FLAIR weighted images are variant of the T2 which are produced by using greater TR and TE than T2. The contrast between different modalities generates the unique image of each tissue. Effective diagnosis of the brain tumor plays important role in the patient's overall survival rate.

Image segmentation is the process dividing an image into well-defined regions or cate-

gories where each area contains pixels with similar attributes and each resolution in an image is assigned to one of these categories [5]. Similarly, Brain tumor segmentation is the process of splitting of tumorous region from the non-tumorous region [6]. Generally, there two types of brain tumor segmentation firstly, the manual decomposition is the tedious and complex task but an accurate meanwhile automatic segmentation is simple as well as accurate due to development in the field of artificial intelligence. Specifically, due to availability of efficient machine leaning algorithms and libraries the application of artificial intelligence in medical imaging is tremendously increasing [7]. Therefore, to utilize the complete benefits of machine learning, a combination of pretrained VGG19 and UNET has been proposed for brain tumor segmentation whereas ensemble voting classifier of Random Forest and Naïve Bayes (NB) was trained for tumorous patient survival prediction. For segmentation, the encoder portion of the UNET is pretrained VGG19 followed by respective decoder part. Whereas for brain tumor survival prediction, data preprocessing steps comprised of feature selection and normalization were proposed followed by ensemble of Random Forest and NB.

1.1 MOTIVATION

According to London Institute of Cancer and World Health Organization there are 18 Million registered cases of cancer globally. Out of which two hundred and ninety thousand cases are brain tumors and the highest cases of brain tumor cases are reported in Asia with the amount of one hundred and fifty six thousand cases. Similarly, 9.5 Million cases of deaths are due to global cancers, of which two hundred and forty one thousand are belongs to brain cancers and the highest mortality rate was observed in Asia with one hundred and twenty nine thousand cases. Meanwhile, Early diagnosis of brain tumors plays essential part in the overall survival of the patient. There are different variations of brain tumor exist which makes it challenging to separate tumorous region from the non-tumorous area, mainly in underdeveloped countries like Pakistan as claimed in different reports, the population is increasing everyday and resources available are inefficient with less experienced professional so there is need of an automated system which is not only accurate but economical as well. Therefore, this research aims to improve the healthcare facility with more accurate and efficient results.

1.2 PROBLEM STATEMENT

Manual diagnosis of the tumor is a difficult job because of non-uniform shapes and complex boundaries. Therefore, this research aims to facilitate medical experts by automatically diagnosing brain tumorous regions using segmentation and segmentation information to predict the overall patient's survival.

1.3 AIMS AND OBJECTIVES

The primary goals of the research are mentioned below:

- To utilize DNN for brain tumorous region segmentation

- To create and train UNET for segmentation

- To use pre-trained VGG19 as encoder part of the UNET

- To utilize segmentation results to build patient survival prediction model

- To train ensemble model for patient survival prediction

- Differentiation of results with prominent detection and prediction techniques

1.4 STRUCTURE OF THESIS

The structure of thesis is followed as:

Chapter 2 describes the basics concepts of Magnetic Imaging Resonance followed by detailed pictures of brain and brain tumor segmentation

Chapter 3 review some previous working for brain tumor segmentation and patient survival prediction and perform deep review of the results achieved

Chapter 4 is the representation of proposed methodologies. Meanwhile, it provides the detail of essential techniques used in the experimentation

Chapter 5 describes the datasets, evaluation matrices and experimentation results are also described in details in this chapter Chapter 6 is the final chapter which concludes the thesis and reveals future scope of the research

FUNDAMENTALS OF MAGNETIC RESONANCE IMAGING AND BRAIN

2.1 ESSENTIAL OF MAGNETIC RESONANCE IMAGING

2.1.1 *Computer Tomography (CT)*

Computed Tomography is a standard diagnostic image modality that uses series of x-ray to build the slices of the body tissues. The CT machine scanners emits an x-ray toward the body from different directions, and detectors in the CT machine measure the variance between x-rays consumed by the body and x-ray diffused from the body. This process is called attenuation [9]. The attenuation is determined by the thickness of the tissues followed by an individual CT number or Hounsfield value. Typically, high thickness tissues fascinate the radiation from a higher degree, and the scanner recognizes a reduced amount on the other side of the body. Conversely, low thickness tissue retains the radiation from the lower point, and a tremendous amount of signal is detected by the scanner. Those tissues with high attenuation coefficient show up white while the tissues with a low attenuation coefficient are shown up as black, quantified by CT number. The CT number or Hounsfield number ranges from -1000 to 1000. For air, the Hounsfield value is -1000, while for bone, the Hounsfield value is 1000. When interpreting a CT
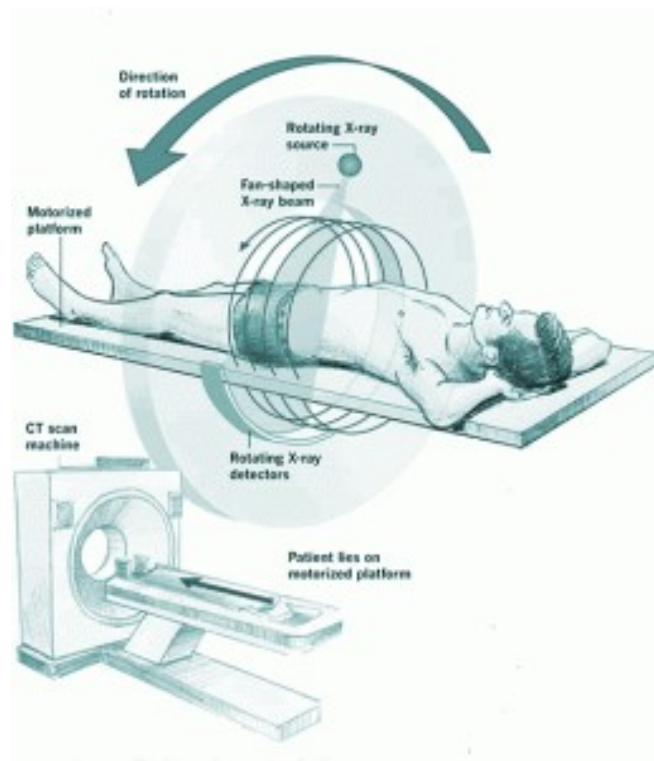
Figure 2.1: Basic Principle of CT [10]

image, the orientation of the image is essential. Usually, images are presented in a transverse plane and are oriented to look up the body from the patient toes. CT image is a digital image consisting of square matric of elements called pixels, and each pixel is represented as a volume element (voxel) of the patient. Figure 2.1 illustrates the basic principle of CT.

2.1.2 *Ultrasound*

Ultrasound is another imaging modality that utilizes sound waves of higher frequency to depict body tissues. It is a more reliable and flexible imaging modality that provides the additional unique characteristics of the tissues. Typically, the frequency of the sound wave in ultrasound ranges from 20 hertz to 20,000 hertz [11]. The ultrasound working is simple: sending an ultrasound wave from the ultrasound transducer into the tissue and receiving echoes back. The echoes contain spatial and contrast information. The ultrasound technique is more sophisticated to gather enough data to generate a two-dimensional grayscale image. In addition to the grayscale image, some characteristics such as the doppler effect of returning echoes can be selected to gather additional
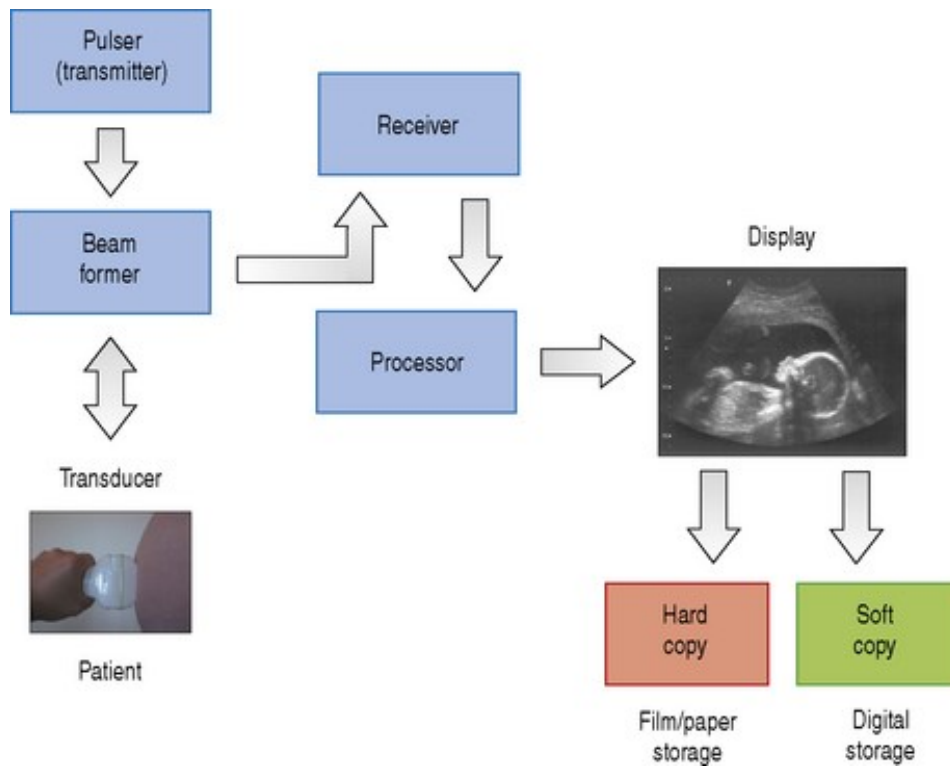
Figure 2.2: Image Acquisition by Ultrasound [12]

information. Ultrasound is a much inexpensive technique than CT. The basic working principle of image acquisition by ultrasound is illustrated in Figure 2.2.

2.1.3 X-Ray
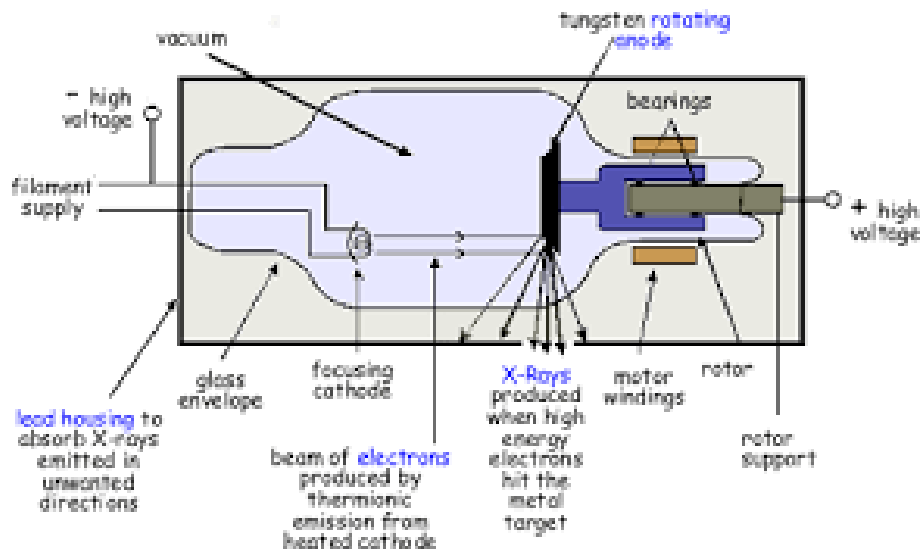
Figure 2.3: The basic principle of X-ray generation [5]

X-ray is the commonly used imaging modality in hospitals. Wilhelm Rontgen initially discovered it in 1895. X-ray is a type of electromagnetic radiation [13]. The radiation is produced when an electric current is created from a high voltage generator. The generator can be an electron, proton, or any other x-ray. It is typically generated by bombarding a metal target with a generator of electrons. The electrons are created by warming a metal filament. The electrons produced from the filament are then moving towards the target material known as an anode. When the generator hits, an anode X-ray is emitted. The x-ray acquisition principle is illustrated in Figure 2.3.

2.1.4 *Magnetic Resonance Imaging*

Magnetic Resonance Image (MRI) allows MRI experts to utilize magnet and radio waves to check inside the human body. MRI scanner was initially developed in 1971 in New York. MRI estimates how much water is in various body tissues by utilizing magnets and radio waves to plan the water's space and uses this information to make a top to bottom picture [14]. The photos are so in-depth because our body is composed of around 65% water. The water molecule (H2O) includes two hydrogen particles and one oxygen atom, as represented in Figure 2.4. The hydrogen (H) atom or the (H) particle is used to figure the sign from the body. At the point when we take a gander at a hydrogen molecule comprehensively, it's anything but a positive charge is procured by a focal core known as a proton. Like the Earth turning on the two poles, the north and the south pole, similarly each rotating protons of hydrogen proton seems like a small magnet pivoting around its own axis'. Like a compass needle changes towards the magnetic field when these are discretionarily turning hydrogen protons are placed in an MRI scanner, their axis realign them with the scanner's more grounded magnetic field. We consider the scanner's magnetic field the B0. Mainly like a compass needle on the earth field, the accurate compass does not move. However, the needle spins to change itself. The hydrogen protons do not truly move in the body when it enters an MRI scanner; their axis essentially changes along the course of the B0 field. Some will change parallel, and some will change anti-parallel to look like while twirling around on their axis. As a result of the laws of quantum physical science, which we will not go into here, there are for each situation just gradually more parallel proton than anti-parallel. If we presently consider the entire magnetic field produced from all our hydrogen protons,
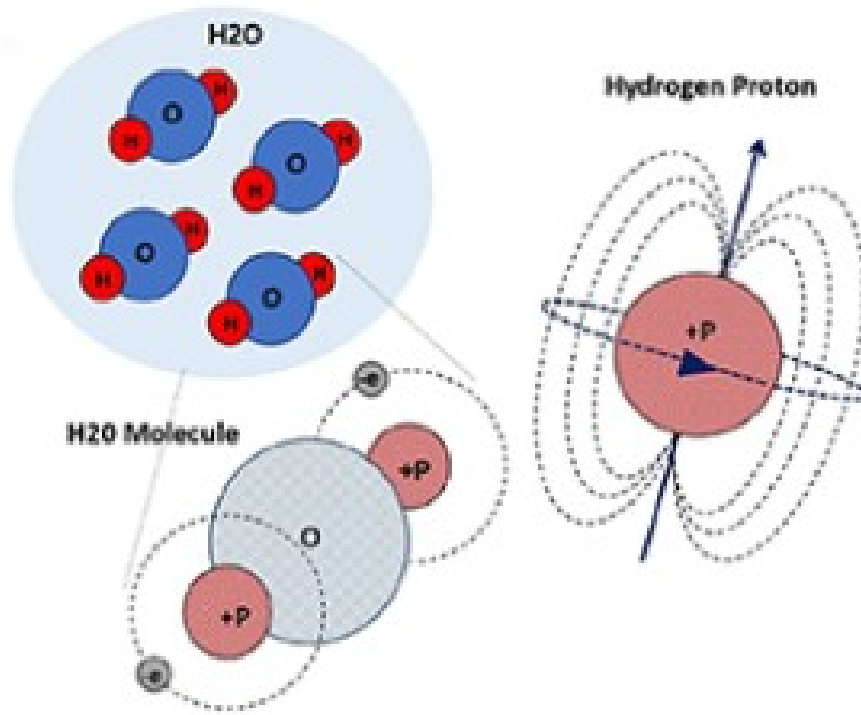
Figure 2.4: H20 molecule

these tiny magnets almost offset each other, to leave simply the magnetic field from the small degree of additional equal protons. It is this bit of magnetic field that we can measure using MRI. The B0 field impacts the hydrogen proton's arrangement plan and impacts how rapidly these protons turn, called precessional frequency. The precessional frequency depends upon the strength of the attractive field. The more grounded the magnetic field, the faster they turn. We get a picture from these turning just by turning hydrogen protons in the cerebrum. The protons turn back and correct alongside the B0. We think about our compass once more when the RF pulse is turned off. The needle will pivot from east to north and line up with the magnetic field again when moving our little bar magnet away. The protons emit energy when they flip back and realigns with B0. Various tissues of the body radiate various amounts of energy. To quantify this radiated energy, we require loop hardware put around the considered part of the body. The loop goes about as a receiving wire and considers as an electrical flow. The electrical flow is changed, through a PC, utilizing a numerical computation called a Fourier transformation. A numerical estimation is utilized to change the electrical flow in a loop into a picture. Since protons in the various types of tissues in mind, like dark matter, white matter, and blood, all radiate various energy measures, the aftereffect

9
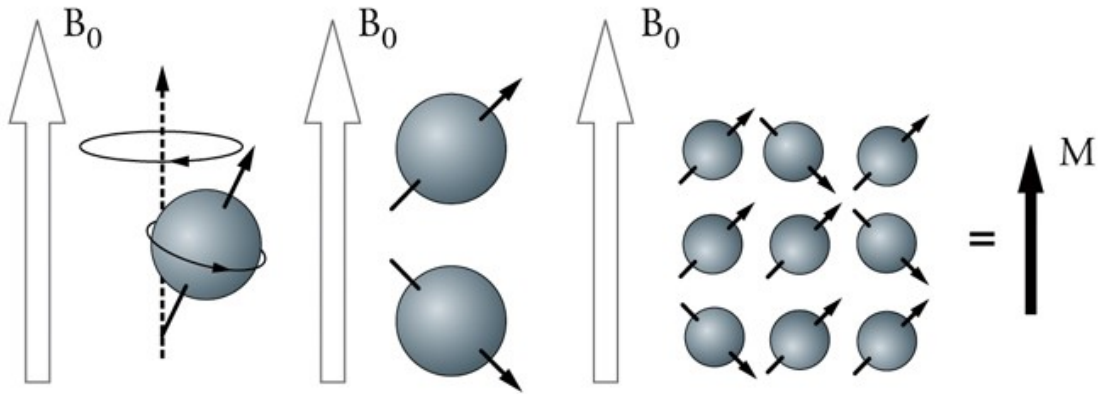
Figure 2.5: Protons in the body

of the changed energy is an exceptionally nitty gritty picture of the tissue inside the cerebrum.

- Relaxation

  Relaxation is the cycle where spin delivered the energy got from a radiofrequency. There are three types of relaxation that influence the MRI signal [15], [16]. T1 relaxation The nuclei spin in the transverse plane and are bounded by the surrounding particles. They do so by returning to the longitudinal magnetization (M) exponentially, as shown in Figure 2.5. The rate at which this happens is represented by a time constant (T1).
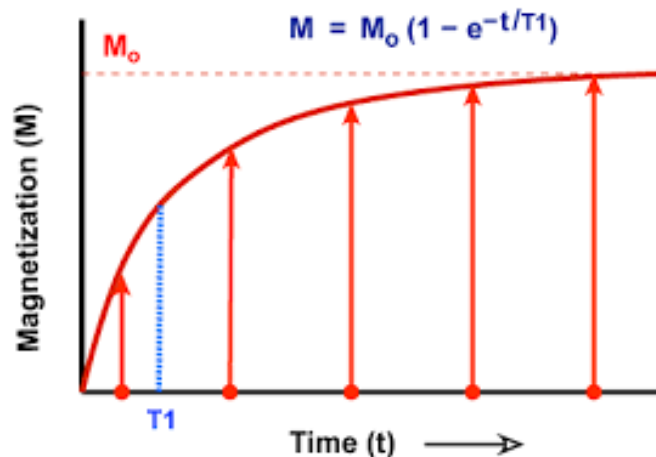
Figure 2.6: MRI exponential curve T2 Relaxation

  T2 relaxation alludes to the advanced dephasing of turning dipoles, bringing about decay in the polarization in the cross-over plane (M). Following a radiofrequency,
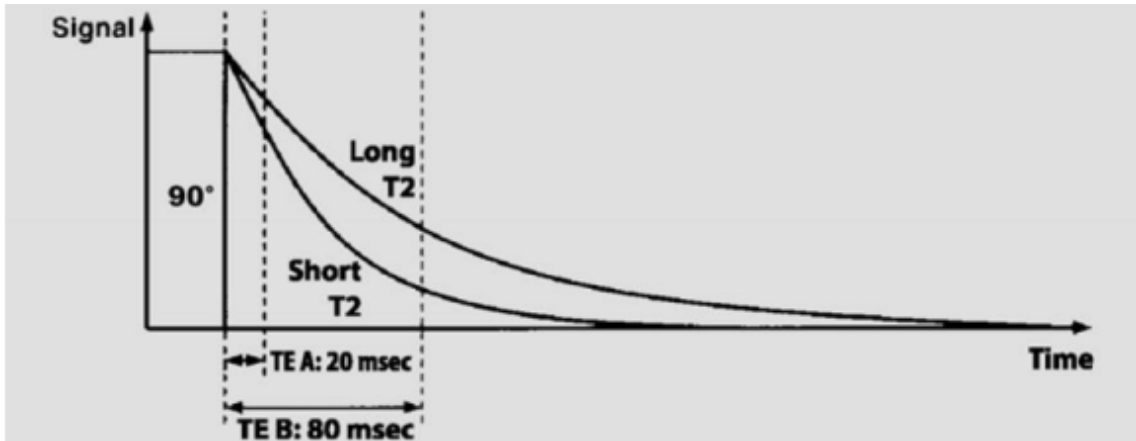
Figure 2.7: Difference between T2 and T2* relaxation

this type of relaxation happens with consistent T2, where T2 is the hour of cross-over polarization vector to rot to 37% of its initial magnitude.

- T2* Relaxation

  T2 relaxation is the exponential curve of transverse decay in the ideal world. However, when we measure it in reality, we track down that the transverse decay is a lot quicker. The signal decreases to zero quicker than expected. This process is called the T2* relaxation.

- Image Contrast

  Three features of biological tissues contribute to the brightness of MRI and enhance overall image contrast. The Proton Density: The proton density determines the maximum signals obtained from a given tissue through an excitable number of spins per unit volume. T1 time of tissue: The T1 time of a tissue is the time that takes the energizing spin to improve and to be accessible for another spin. T1 sign can be fluctuated haphazardly and influences the sign power by implication. Contrast images that the T1 determines are called T1 weighted images. T2 time of tissue: It determines the fades out of the MRI signal after excitation. The operator can control the T2 contrast of MRI. Contrast images that the T2 determines are called T2 weighted images [17].

- Spatial Encoding and Slice Selection

  MR imaging produces cross-sectional pictures of the human body. Therefore, the excitation pulse is conveyed uniquely to the slice we need to imagine and not the
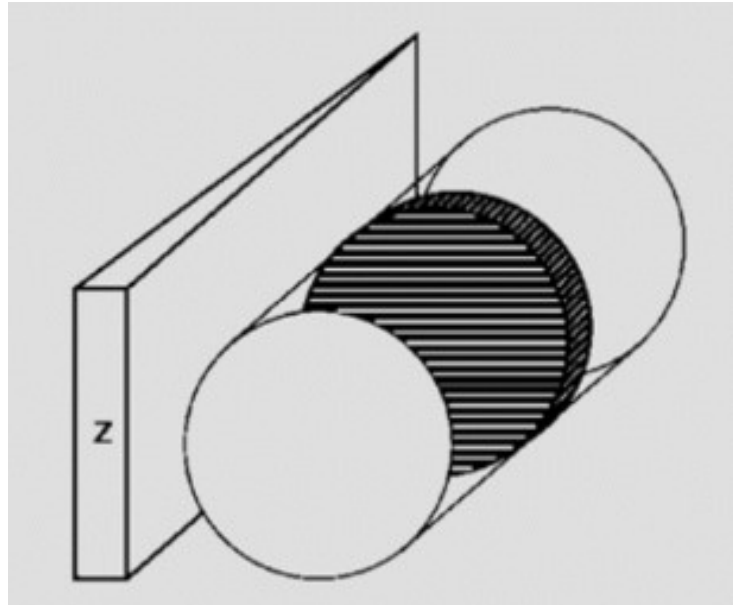
Figure 2.8: Slice selection in the z-axis

entire body [18]. Allow us to consider a cross-over (hub) slice or get segment through the body. The magnetic field created by most MR scanners is not guided through, however, along with the body slice of the individual being imaged. This is the course assigned by "z" since, as of now said, z represents the bearing of the primary magnetic field. The magnetic field angles that presently become an essential factor are addressed by wedges, with the tip represents the lower field strength, and the thick side represents the higher field strength.

- K-Space
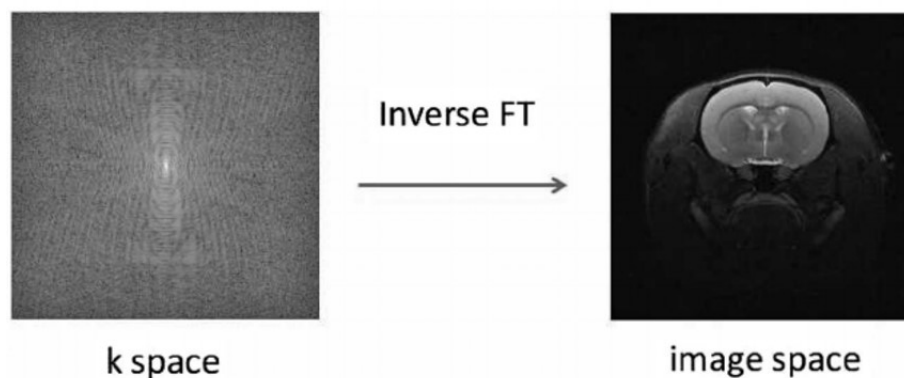
Figure 2.9: MRI generation from k-space MRI Modalities

The spatial data obtained from the MRI scanner is transformed to the frequency

domain during the acquisition process. In the MRI, the initial encoded acquired data is referred k-space. They are Fourier-transformed data [19]. To convert back to spatial information, apply the inverse Fourier transform to obtain the MR image. Each data point in the k-space is derived directly from the MR signal. Inverse FT is applied after k-space acquisition to gain the final image. Each pixel in the achieved image is the total sum of all the discrete points in the k-space. The Figure 2.9. illustrate the generation of MRI from k-space
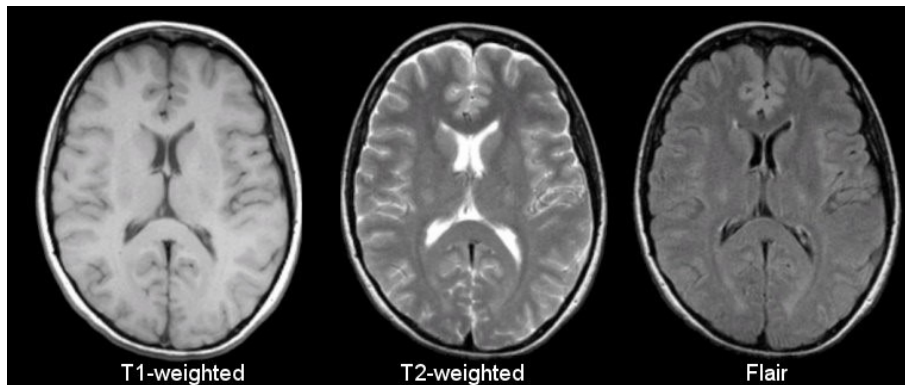
Figure 2.10: Comparison of T1-weighted Image with T2-weighted and Flair [20]

There are three most common types of MRI modalities. The modalities are classified based on Time to Echo (TE) and Repetition Time (TR). T1-Weighted images: are generated by using short TE and TR times. The T1 properties of tissue determine the brightness and contrast of the T1-weighted image. T2-Weighted images: are created by utilizing longer TR and TE times. The T2 properties of tissue determine the brightness and contrast of the T1-weighted image. Flair Attenuated Inversion Recovery (FLAIR): is another most common type of MRI modality and is similar to T2-weighted images by having a significantly longer TE and TR modality. The cerebral spinal fluid (CSF) is bright on T2-weighted imaging and dark on T1-weighted imaging, as shown in Figure 2.10.

To summarize, MRI can be generated in the following five steps: The MRI scanner emits an RF pulse at a specific frequency RF coil sends the pulse to the examined area of the body The RF pulse is consumed by protons, making their redirection for the essential magnetic field When the RF pulse is turned off, the protons rotate back to the initial position by emitting radio waves Finally, the spatial information is converted to measured data in the frequency domain

2.2 STRUCTURE OF BRAIN

The structure of the brain is composed of three main parts, which is illustrated in Figure 2.11 with their functionality; The forebrain is composed of the cerebrum. The cerebrum is the central segment of the brain. It is responsible for the higher functionality of the cerebral, such as action and thought. The forebrain is divided into four subsections called lobes. The midbrain is smallest segment of the brain located below the cerebrum and above the hindbrain, and it is also located almost centrally within the cranial cavity. It comprises the cerebral peduncles, several nuclei, fasciculi, tegmentum, cerebral aqueduct, and tectum, The fundamental occupation of the midbrain is to fill in as a kind of relay station for our auditory and visual systems. Sections of the midbrain called the red center and the substantia nigra are locked in with the control of body advancement. The hindbrain is a region made out of the medulla oblongata, the pons, and the cerebellum. The hindbrain facilitates capacities that are crucial to survival, including respiratory beats, motor action, rest, and alertness.
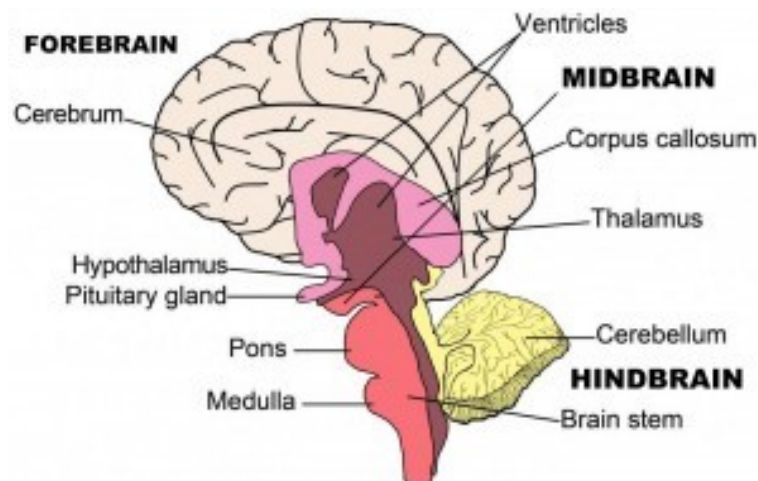
Figure 2.11: Structure of Brain [21]

2.3 Segmentation of Brain Tumor

Essential brain tumors start in the cerebrum and happen due to strange synapses, known as mutations. As the cells mutate, they develop and duplicate wildly, shaping a tumor. Malignancies that have spread to the mind from different areas in the body are known as cerebrum metastases.

Image segmentation states dividing an image into distinct regions or categories, with each region containing pixels with similar attributes and each pixel in an image being allocated to one of these categories. Similarly, the process of using an MRI scan to find a tumor is called Brain Tumor Segmentation. The goal of Segmentation of Brain Tumor is to separate the non-tumorous region from the tumor region as the brain tumor borders are hard to detect from an MRI scan. This is performed by detecting atypical areas when compared to typical tissue.
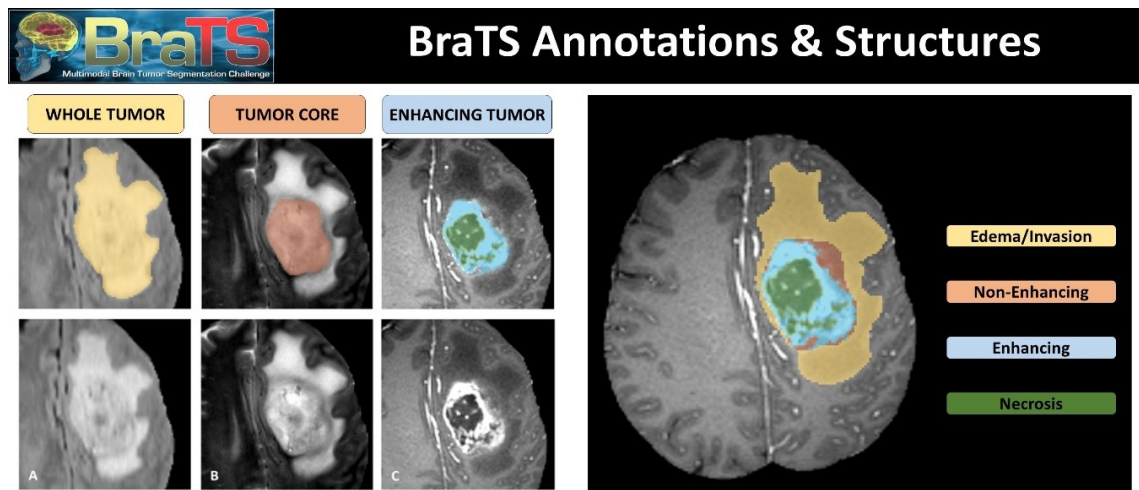
Figure 2.12: (A) The visibility of WT in FLAIR (B) The visibility of TC in T2 (C) The visibility of structure of enhancing tumor as blue in T1C, nearby the cystic/necrotic components of the core as green (D) Segmentations are joint to create the final labels of the tumor [23]

The rule for interpreting the various pictorial structures is illustrated in [22] for low and high-grade cases illustrated in Figure 2.12. T2 images were used to segment edema. In the resulting steps, The relabelled part of the core structure contains the underlying "edema" segmented in T2 and FLAIR, as showing in Figure 2.12 (A). The segmentation of both non-enhancing tumors and enhancing was first segmented by assessing hyper-intensities in T1C and the hypotensive areas noticeable in T1, as shown in Figure 2.12 (B). The proper intensity threshold was resolved outwardly dependent upon the situation shown in Figure 2.12 (C). The necrotic or core was low-intensity necrotic structures inside the enhancing border observable in T1c illustrated in Figure 2.12 (C). Finally, the segmentation are integrate to create final labels of all tumor types are illustrated in Figure 2.12 (D).

Chapter Summary

In this chapter, a complete working of MRI along with different MRI modalities are described with some basic knowledge of other medical imaging modalities. Specifically, a briefly depiction of how magnetic fields shift the control of water molecules in the human body and various tissues react differently to RF pulse. Meanwhile, the structure of brain and segmentation of brain tumor is also discussed briefly.

LITERATURE REVIEW

3.1 BRAIN TUMOR SEGMENTATION

Havaei et al. [24] proposed efficient, flexible, and high capacity DNNs consist of Local and global pathways of 7x7 and 13x13 respective fields for Segmentation of Brain Tumor. Similarly, three different variants of cascaded architectures on the basis of connecting the output of the initial layer to the input of different hidden layers of architectures were also proposed. The experimentation of the proposed method was performed on MRI datasets of Segmentation of Brain Tumor datasets (BRATS 2013). The evaluation metrics used in the experiment were dice, sensitivity, and specificity. The dice score of two pathway architecture is between 70 and 80 percent. The sensitivity and specificity were between 70 to 90%. Then, the dice score of cascaded-based methods was between 70 and 90%, and sensitivity, specificity was between 75 to 85 and 70 to 90 percent, respectively. Similarly, Pereira et al. [25] proposed a CNN and tunning the intensity normalization transformation for low-grade and high-grade gliomas segmentation. The validation of the proposed method was performed on BRATS 2013 and 2015 of MRI datasets. Dice similarity score on BRATS 2013 was 0.88, 0.83, and 0.77 for complete, core, and enhancing brain regions, respectively. Similarly, the DSC on BRATS 2015 were 0.78, 0.65, and 0.75 for WT, CT, and ET, respectively. Zhao et al. [26] proposed an accurate and faster slice by slice brain image segmentation for tumor detection consist of three steps. Firstly, training FCNN using image patches, then training CRF-RNN using image slices, and finally, Fine-tune FCNN and CRF-RNN using image slices. The efficiency of the proposed method was performed on BRATS 2013, BRATS 2015, and

BRATS 2016. The evaluation metrics used in the experiments were Dice score, Positive predictive value (PPV), and sensitivity. The dice score, PPV, and sensitivity were between 0.75 and 0.90 for each mode of the MRI. A fully automated end-to-end incremental CNN model for MRI Segmentation of Brain Tumor was proposed by Saouli et al. [27]. Specifically, 2CNet, 3CNet, and EnsembleNet methods were proposed. These models exploit local and global features of the patches using two pathways. The evaluation of proposed methods was performed on BRATS 2017. The dice score and sensitivity of 2CNET, 3CNET, and EnsembleNet were between 0.8 and 0.9. Similarly, the specificity of 2CNET, 3CNET, and EnsembleNet was between 0.75 and 0.9. Zhao et al. [28] proposed an efficient FCNN for 3D Segmentation of Brain Tumor. The proposed integration of three 2D FCNNs and each 2D FCNNs were trained to segment brain images from axial, coronal, and sagittal view, respectively. The evaluation was performed on BRATS 2017. The maximum dice score of the proposed method was between 0.82 to 0.92, and PPV was between 0.81 to 0.92. Similarly, sensitivity was between 0.82 to 0.88 for all the modes of MRI. Colmeiro et al. [29] proposed a simple and fast 3D UNET method for automatic Segmentation of Brain Tumor. Specifically, two steps 3D DCN was proposed. In first step, whole tumor was segmented from low resolution volume then the second step was to make fine tissue segmentation. The proposed method was evaluated on BRATS 2017 datasets and the maximum dice score, sensitivity, specificity and Hausdorff distance mean on unseen datasets was 0.86, 0.997 and 14.0 for whole, enhanced and core region respectively. Similarly, a UNET consist of 23-layer deep FCNN for fully automated voxel-based segmentation of gliomas was proposed by Alex et al. [30]. The proposed method was trained and validated on BRATS 2017 datasets and the dice score on whole tumor, core tumor and active tumor were 0.79, 0.65 and 0.63 respectively. Similarly, Myronenko et al [35] proposed a 3D MRI brain tumor semantic segmentation using encoder-decoder architecture. Specifically, a variational auto-encoder was used to construct input image and decoder was used to impose constraints on its layer. The proposed method was evaluated on BRATS 2018 and the maximum Dice scores value for enhance, whole and core tumor were 0.82, 0.91 and 0.86 respectively. Similarly, Hausdorff distances for enhance, whole and core tumor were 8.0, 10.0 and 5.9 respectively. Li et al. [32] proposed an ensemble of CNN and fully connected conditional random field (CRF) in two steps. In the first step, 3D MRI is input to CNN for accurate recognition of glioma. Then the output is applied to CRF for boundaries description. The private

datasets used in this experimentation were obtained from Shanghai Huashan Hospital. The datasets are composed of 59 training sets and 101 test sets. The maximum Dice similarity coefficient (DSC), positive predictive value (PPV), and sensitivity on training sets were 0.85, 0.83, and 0.88, respectively. Similarly, the maximum Dice similarity coefficient (DSC)], positive predictive value (PPV), and sensitivity on test sets were 0.85, 0.85, and 0.86, respectively. Soltaninejad et al. [31] proposed a learning-based method for automatic Segmentation of Brain Tumor into multimodal images. Specifically, FCNN was used to extract features from MRI. The Random Forest (RF) was used to classify MRIs into typical and different kinds of tissues. The proposed method was validated on BRATS 2017. The mean dice score on the whole tumor, core tumor, and active tumor were 0.86, 0.78, and 0.66, respectively, unseen data. Similarly, integration of FCNN and CRF for Segmentation of Brain Tumor was proposed by Zhao et al. [33]. The proposed method consists of three steps. In the first step, MRI is input to FCNN for training. The output of FCNN was used to train CRF, and in the last step, image slices obtained from CRF were used to fine-tune the whole network. The performance of the proposed method was evaluated on BRATS 2013, and the maximum Dice similarity coefficient (DSC)], positive predictive value (PPV), and sensitivity were achieved on the whole region, i.e., 0.87, 0.92, and 0.83, respectively. Chang et al. [34] proposed an efficient and robust fully convolutional residual neural network (FCR-NN) was proposed for tumor segmentation. FCR-NN gain optimization from residual identity and combine with CNN. The proposed method was validated on BRATS 2016. The Dice scores value for complete, core, and enhancing tumor were 0.89, 0.83, and 0.78, respectively. The Hausdorff distances for complete, core, and enhancing tumors were 8.0, 10.0, and 5.9, respectively. Similarly, McKinley et al. [36] proposed an ensemble of multiple classifiers based on DeepSCAN. The architecture consists of densely connected blocks of dilated convolutions following the UNET structure. The validation of the proposed method was performed on BRATS 2018. The mean Dice scores value for enhancing ,whole and core tumor were 0.73, 0.88 and 0.79. Similarly, Hausdorff distances for enhancing, whole, and core tumors were 3.4, 5.51, and 5.53, respectively. Isensee et al. [37] proposed the context pathway of UNET combines high-level features and is subsequently localized with the localization pathway of UNET. The validation was performed on BRATS 2017. The dice score on validation datasets was 0.896, 0.797 and 0.732 for the WT, TC and ET, respectively. Similarly, dice score on test sets was 0.858, 0.775, and 0.647 for

whole, core, and enhancing tumors. Chen et al. [38] proposed an efficient 3D CNN for real-time segmentation. Similar to UNET, a multi-scale representation was achieved in the encoding stage by applying Dilated Multi-Fiber (DMF) for the encoding unit. Then in the decoding stage, the high-resolution feature was combined with upsampling for final segmentation. The effectiveness of the proposed method was evaluated on BRATS 2018 with dice scores of 0.812, 0.90, and 0.84, respectively, for the ET, WT and TC. Similarly, Lachinov et al. [39] proposed the modification of UNET. Precisely, the proposed network consists of three UNET building blocks. The output of one block is the input to the next block, which takes down-sampled volume as input and produces the segmented image. The dataset used in the experiments was BRATS 2018, with a mean Dice score of 0.908, 0.784, and 0.844 was obtained on the validation dataset for the WT, ET and TC, respectively. Li et al. [40] proposed a GAN-based approach for Segmentation of Brain Tumor. The generator follows an adversarial process and discriminator to generate synthetic images from the generator's output. The proposed method was evaluated on BRATS 2017 datasets. The dice score, PPV, and sensitivity of the whole and core region were between 86 and 89. Similarly, dice score, PPV, and sensitivity of enhancing area were between 77 and 78. Similarly, Rezaei et al. [41] proposed a CGAN for Segmentation of Brain Tumor. A generator was an FCN encoder-decoder that generates probability mapping from input to multi-model images. The discriminator was a binary classifier that maps the predicted mask from the segmented network. The evaluation of the proposed method was performed on BRATS 2017 datasets, with the maximum dice score on validation datasets was 0.8. Similarly, maximum sensitivity, specificity, and Hausdorff distance on validation datasets were 0.75, 0.99, and 12.04. Again, a GAN-inspired Segan was proposed by Xue et al. [42] for Segmentation of Brain Tumor. Specifically, the segmented network of Segan is a convolutional encoder-decoder that maps probability labels to an input image. The discriminator network was used to predict the label to segment network. The effectiveness of the proposed method was validated on BRATS 2013 and BRATS 2015 with maximum Dice similarity coefficient, precision, and sensitivity for BRATS 2013 on the whole region were 0.84, 0.87, and 0.83, respectively, and the leading Dice similarity coefficient, accuracy, and sensitivity for BRATS 2015 on the entire area were 0.85, 0.92 and 0.8 respectively. Recently Cirillo et al. [43] proposed a Vox2Vox, a voxel-to-voxel GAN-based framework for segmentation. The generator network of Vox2Vox is the enhancement of 3D UNET, while the

discriminator is the 3D CNN for determining the quality of an image generated by the generator. The proposed method was evaluated on BRATS 2020, with the mean Dice scores value for enhancing, whole and core tumor on training datasets were 0.79, 0.91, and 0.89, respectively. Similarly, Hausdorff distances for enhancing, whole and core tumors were 30.04, 3.52, and 3.66, respectively. Khosravanian et al. [44] proposed a Segmentation of Brain Tumor approach based on superpixel fuzzy clustering and the lattice Boltzmann method. Specifically, a three-step segmentation process was presented. Level set equations are also obtained using the gradient descent method. Finally, a level set equation was achieved by using the lattice Boltzmann machine. The performance of the proposed method was evaluated on BRATS 2017 datasets, and the average Dice and Jaccard coefficient was 0.93 and 0.87, respectively. Khan et al. [45] proposed a deep learning approach with MRI data analysis to classify the brain. Specifically, the process comprises three phases. In the first phase, MRI preprocessing was performed. K-mean clustering was applied for Segmentation of Brain Tumor, and finally, VGG19 was applied to perform tumor classification. The BRATS 2015 datasets were used in the experimentation with a classification accuracy of more than 90%. Chen et al. [46] proposed a variant of Deep Convolutional Neural Network (DCNN) called Deep Convolutional Symmetric Neural Network which only adds symmetric masks in several layers in DCNN for Segmentation of Brain Tumor. The validation of proposed method was performed on BRATS 2015 with Dice Coefficient Score of 0.852. Zhou et al. [47] proposed an ERV-Net for segmentation of tumor. In ERV-Net, a 3D ShuffleNetV2 was utilized as encoder part, and Residual Block was taken as decoder part of the UNET. Effective post-processing was applied to enhance the segmentation output. The validation of processing was performed on BRATS 2018 with a Dice score of 81.8%, 91.21%, 86.62%, for ET, WT, and CT, respectively. Pei et al. [48] proposed two methods for segmentation. The first method combine stochastic multi-resolution texture features with cell density component. The second method utilizes the joint label function (JLF) to combine labels obtained from stochastic texture feature-based, Random Forest (RF), and boosted Glioma Image Segmentation and Registration (GLISTRboost). The evaluation is performed on BRATS 2015 with an average dice score of 0.4 and 0.82 for both methods. Similarly, Naser et al. [49] proposed a pre-trained VGG16 with UNET for Segmentation of Brain Tumor. The datasets used in the experimentation were BRATS 2013 and BRATS 2015. The mean dice similarity coefficient and tumor detection accu-

racy achieved by the segmentation are 0.84 and 0.92. Zeineldin et al. [50] proposed a deep learning model called as DeepSeg for segmentation. Specifically, DeepSeg is modified from UNET with Residual neural Network (ResNet), Dense convolutional network, and NASNet as an encoder part of UNET. The efficacy of the proposed method was performed on BRATS 2019 with dice and Hausdorff score of 0.81, 0.84, and 9.8 and 19.7, respectively. Zeineldin et al. [51] applies different pretrained deep learning architecture for fully automatic segmentation. Similar to conventional U-NET, an encoder is a CNN responsible for feature extraction followed by respective decoder part to achieve the semantic probability map. Specifically, different CNN model such as DenseNet, ResNet and NASNet was utilized as encoder. The evaluation of proposed method was performed on BRATS'19 datasets and achieved a dice coefficient score (DSC) of 0.839, 0.837, 0.839, and 0.835 on Xception, VGGNet, DenseNet, and MobileNet encoder respectively. Pei et al. [52] proposed a context aware deep neural network (CANet) framework for brain tumor segmentation. In addition to encoder and decoder part of U-NET, it has context encoding module which computes scaling factors of all classes. These scaling factor learns the global representation of all tumor classes. The validation of proposed method was performed on BRATS'19 and BRATS'20 dataset and evaluation metrices used in the experimentation was DSC. The DSC on test set were 0.821, 0.895, and 0.835 for ET, WT and TC respectively. Ghosh et al. [53] proposed a pretrained deep learning architecture for brain tumor segmentation. The proposed architecture is similar to standard UNET except the encoder part is pretrained VGG16 which consist of 13 convolutional layers, 5 pooling layers and 3 fully connected layers therefore decoder also have 13 convolutional layers, 5 up sampling layers and 3 fully connected layers. The validation of proposed method was performed on The Cancer Imaging Archive (TCIA) and evaluation was performed on different metrices such as accuracy, DSC, and intersection over Union (IoU). The accuracy, DSC, and intersection over Union (IoU) of proposed method is 0.998, 0.93 and 0.83 respectively. Alqazzaz et al. [54] trained a variant of Segnet for brain tumor segmentation. Specifically, four different SegNet were trained on T1, Flair, T1ce and T2 weighted images. Then four SegNet combine each other and feature extraction is performed and finally Decision Tree was applied on extracted features to generate the predicted segmentation mask of tumor region. The datasets used in the experimentation was BRATS'17 and evaluation metrices were precision, recall and F-measure and achieved the F-measure of 0.85, 0.81 and 0.79 on whole, enhancing and

core tumor respectively. Kaewrak et al. [55] proposed an encoder-decoder deep neural network for multi class brain tumor segmentation. The proposed architecture is called as TwoPath U-NET because it learns both local and global features by uses local and global feature extraction path in down-sampling path of the deep neural network. The validation of proposed method was performed on BRATS'19 and dice coefficient score was the evaluation metrices used in the experimentation. The dice coefficient score of proposed method was 0.76, 0.64 and 0.58 for whole tumor, enhancing tumor and core tumor respectively. Silva et al. [94] presented a deep multi cascade fully connected neural network for brain tumor segmentation. Specifically, the proposed architecture is composed of cascaded of three deep layer aggregation neural network i.e., basic convolutional block, convolutional block and aggregation block. The evaluation of proposed method was performed on BRATS'20 datasets and DSC and Hausdorff distance were the evaluation metrices used in the experimentation. The DSC was 0.88, 0.82 and 0.79 for WT, TC and ET respectiveLY. Murugesan et al. [95] presented a multidimensional and multiresolution ensemble neural network for brain tumor segmentation and trained traditional machine learning model for survival prediction. Specifically, an ensemble of pretrained neural networks such as DenseNET-169, SERESNEXT-101 and SENet-154 were utilized to segment WT, TC and ET respectively. Then the segmentation map was produced by combining segmentation of ensemble of pretrained deep neural networks. The datasets used in the experimentation was BRATS'19 and achieve dice coefficient score of 0.89, 0.78 and 0.779 for WT, TC and ET respectively and survival prediction accuracy was 34Qamar et al. [96] trained a 3D UNET to classify the tumor into whole tumor, enhancing tumor and core tumor classes. Specifically, the proposed architecture extracts the multi-stake information by combining information of 3D convolutional neural network in the residual inception block and by utilizing hyperdense inception 3D UNET. The validation of proposed method was performed on BRATS 2020 datasets and achieve the dice coefficient score of 0.79, 0.87 and 0.83 for ET, WT and TC respectively. Zhuge et al. [97] presented a holistically nested neural network for the segmentation of brain tumor. The multiscale and multilevel hierarchical features of the brain MRI was learned by the holistically nested neural network which is the extension of CNN to generate the prediction map of test images of brain MRI. The evaluation of proposed method was performed on BRATS'13 datasets and evaluation metrices used in the experimentation were DSC and sensitivity. The achieve results shows that the

presented method outperformed the previous method with DSC and sensitivity of 0.83 and 0.85 respectively. Cui et al. [98] proposed a cascaded convolutional neural network for brain tumor segmentation. The proposed architecture is composed of two subnetworks. First network is called as tumor localization network (TCN) and it is used to detect the tumorous region from MRI scan. The second network was called as intratumor classification network (ITCN) which was used to label the defined tumorous region into sub regions. The proposed architecture was validated on BRATS'15 datasets and DSC, sensitivity and Positive Predicted Value (PPV) are the evaluation metrices used in the experimentation and achieve DSC of 0.89, 077 and 0.80 for WT, TC and ET respectively. Kamnitsas et al. [14] proposed an Ensemble of Multiple Model and Architecture (EMMA) for efficient brain tumor segmentation for determining the influence of meta-parameters on individual model while reducing the risk of overfitting. Specifically, the proposed architecture is the ensemble of two 3D multi-scale CNN called DeepMedic, Fully Connected Network (FCN) and UNET. The performance of proposed architecture was validated on BRATS'17 which consist of 215 High Grade Glioma (HGG) images 75 Low Grade Glioma (LGG) images. The DSC of 72.9, 88.6 and 78.5 were obtained for ET, TC and WT respectively

3.2 SURVIVAL PREDICTION

Agravat et al. [56] apply Random Forest Regression (RFR) with five-fold cross-validation for the tumor's overall survival prediction. The performance of RFR has been evaluated on BRATS 2020 datasets which consist of Age, volume, and shape features. The RFR achieve an accuracy of 56.8% and 51.7% on the training and validation set, respectively. Similarly, Anand et al. [57] extracted 1022 features from BRATS 2020 datasets. Only 32 most important components are selected, and finally, RFR was applied to selected features. The proposed method achieved an accuracy of 44.8% and 44.52% on validation and test set. Kao et al. [58] proposed a three-step process for the survival prediction of a patient. In the first step, an ensemble of lesion occurrence probabilities in structural regions with MR images and a patch-based neural network was proposed for the Segmentation of Brain Tumor. Then, feature normalization and feature selection were performed. Finally, the SVM was applied to selected features for overall survival prediction. The BRATS 2018 datasets were utilized in the experimentation and achieved an

Table 3.1: Summary of BRATS on 2013 datasets

Ref.#	Proposed Method	Goal	Results
[24]	Local and global pathway consist of 7x7 and 13x13 respective field for Segmentation of Brain Tumor. Similarly, three different variants of cascaded architectures based on the mapping of output of first layer to the input of different hidden layers of architectures were proposed	An efficient, flexible and high capacity DNNs for Segmentation of Brain Tumor	The dice score of two pathway architecture is between 70 and 80 percent. Similarly, dice score of cascaded based methods was between 70 and 90%
[40]	Integration of FCNN and CRF for Segmentation of Brain Tumor was proposed. In first step, MRI is input to FCNN for training then output of FCNN was used to train CRF and in last step image slices obtained from CRF were used to fine tune the whole network	Novel and accurate automatic method for Segmentation of Brain Tumor	The maximum DSC, positive predictive value (PPV), and sensitivity were achieved on complete region i.e., 0.87, 0.92 and 0.83 respectively
[33]	Two steps 3D DCN was proposed for Segmentation of Brain Tumor. In first step, whole tumor was segmented from low resolution volume then the second step was to make fine tissue segmentation	A simple and fast 3D UNET method for automatic Segmentation of Brain Tumor	The mean dice score on unseen datasets was 0.86 whole, whole, enhanced and core region respectively

Table 3.2: Summary of BRATS on 2017 datasets

Ref.#	Proposed Method	Goal	Results
[27]	2CNet, 3CNet, EnsembleNet methods were proposed based on CNN. These models exploit local and global features of the patches using two pathways	A fully automated end-to-end incremental CNN models for MRI Segmentation of Brain Tumor	The dice score and sensitivity of 2CNET, 3CNET and EnsembleNet was between 0.8 and 0.9
[28]	Integration of three 2D FCNNs and each 2D FCNNs were trained to segment brain images from axial, coronal and sagittal view respectively	Proposed efficient FCNN for 3D Segmentation of Brain Tumor	The maximum dice score of proposed method was between 0.82 to 0.92 and PPV was between 0.81 to 0.92
[47]	GAN based approach for Segmentation of Brain Tumor where generator follows adversarial approach and discriminator was used to generate synthetic image from the output of generator	An efficient CNN for Segmentation of Brain Tumor to increase the spatial contiguity	The dice score, PPV and sensitivity of complete, Core region and enhancing region was between 0.79 and 0.88
[48]	CGAN for Segmentation of Brain Tumor where generator was FCN encoder-decoder that generates probability mapping from input to multi model images and discriminator was binary classifier that maps predicted mask from segmented network	An efficient, automatic end to end CNN for semantic Segmentation of Brain Tumor	The maximum dice score and Hausdorff distance on validation datasets was 0.8. and 0.75 respectively

Table 3.3: Summary of BRATS on 2018 datasets

Ref.#	Proposed Method	Goal	Results
[35]	3D MRI brain tumor semantic segmentation using encoder-decoder architecture. A variational auto-encoder was used to construct input image and decoder was used to impose constraints on its layer	Sematic segmentation network for brain tumor detection	The maximum Dice scores value for enhance, whole and core tumor were 0.82, 0.91 and 0.86 respectively
[36]	Ensemble of multiple classifiers based on DeepSCAN were proposed for Segmentation of Brain Tumor. The architecture consists of densely connected blocks of dilated convolutions following UNET structure	Multiple classifiers for Segmentation of Brain Tumor	The mean Dice scores value for enhance, whole and core tumor were 0.73, 0.88 and 0.79 respectively
[38]	Similar to UNET, in encoding stage a multi scale representation was achieved by applying Dilated Multi-Fiber (DMF) for encoding unit then in decoding stage, high resolution feature was combined with up sampling for final segmentation	The effectiveness of proposed method was evaluated on BRATS 2018	The dice scores of 0.812, 0.90 and 0.84 respectively for the enhancing tumor, the whole tumor and the tumor core
[39]	The proposed network consists of three UNET building blocks. The output of one block is the input to next block which takes downsampled volume as input and produce segmented image	Modification of UNET for Segmentation of Brain Tumor	The mean Dice score of 0.908, 0.784 and 0.844 was obtained on validation dataset for the WT, ET and CT respectively

Table 3.4: Summary of BRATS on different datasets

Ref.#	Proposed Method	Goal	Results
[40]	Firstly, training FCNN using image patches then training CRF-RNN using image slices and finally, Fine tune FCNN and CRF-RNN using image slices	Accurate and faster slice by slice brain image segmentation for tumor detection	The dice score, PPV and sensitivity were between 0.75 and 0.90 for each mode of the MRI
[32]	Ensemble of CNN and fully connected conditional random field (CRF). IN first step, 3D MRI is input to CNN for accurate recognition of glioma then output is applied to CRF for boundaries description	Multiple classifiers for Segmentation of Brain Tumor	The maximum DSC, positive predictive value (PPV), and sensitivity on test sets were 0.85, 0.85 and 0.86 respectively
[42]	The segmentor network of SegAN is convolutional encode-decoder that maps probability labels to input image. The discriminator network was used to predicted label to segmentor network	An encoder-decoder based method for Segmentation of Brain Tumor	The maximum Dice similarity coefficient, precision and sensitivity on complete region were 0.85, 0.92 and 0.8 respectively

28

average accuracy of 63%. Puybareau et al. [59] proposed a pre-trained VGG-16 network for Segmentation of Brain Tumor. Then ten most relevant features were extracted from the datasets. Finally, the Random Forest algorithm was applied for overall survival prediction. The dataset used in the experimentation was BRATS 2018.

Shboul et al. [60] proposed a state-of-the-art method for overall survival prediction. Specifically, an ensemble of multiclass Random Forest (RF) and CNN-based tumor segmentation was proposed for Segmentation of Brain Tumor. Then, a total of 1207 features were extracted from datasets. Finally, RF was applied to predict the patient's survival. The overall accuracy of 63% was achieved on BRATS 2017. Feng et al. [61] proposed an ensemble deep learning model for Segmentation of Brain Tumor. Then six most important features were extracted from segmentation results. Finally, multivariate linear regression was trained to predict the overall survival prediction. The dataset used in the experimentation was BRATS 2018. The maximum accuracy of the proposed method was 61%. Zhao et al. [62] proposed a deep learning model called segmentation then Prediction (STP) for Segmentation of Brain Tumor and overall survival prediction. Specifically, a 3D UNET and a 3D ResNET-50 were proposed for local and global feature extraction. The validation of the proposed method was performed on BRATS 2020 datasets and achieved an accuracy of 65.5% for survival prediction. Ali et al. [63] proposed an ensemble model of 2D and 3D Convolutional Neural Network (CNN) for Segmentation of Brain Tumor. Then multiple radiomic and image-based features were extracted from MRI images and segmented regions. Finally, a classification algorithm was applied to predict the overall survival of the patient. The performance of the proposed method was validated on BRATS 2020 and achieved an accuracy of 57% for survival prediction.

Table 3.5: Summary of Survival Prediction on different datasets

Ref.#	Proposed Method	Datasets	Results
[57]	Extract 1022 features from BRATS 2020 datasets then only 32 most important features are selected and finally RFR was applied on selected features	The validation of proposed method is performed on BRATS 2020	The proposed method achieved an accuracy of 44.8% and 44.52% on validation and test set respectively
[58]	A pretrained VGG-16 network for Segmentation of Brain Tumor. Then 10 most relevant features were extracted from datasets and finally Random Forest algorithm was applied for overall survival prediction	The BRATS18 datasets was used in the experimentation	The prediction accuracy of proposed method was 58%
[59]	Six most important features were extracted from segmentation results and finally multivariate linear regression was trained to predict the overall survival prediction	The BRATS18 datasets was used in the experimentation	The classification accuracy of proposed method was 61%
[60]	A 3D UNET and a 3D ResNET-50 was proposed for local and global feature extraction	The performance of proposed method was validated on BRATS20 datasets	The survival prediction accuracy of proposed method was 65.7%

METHODOLOGY

4.1 INTRODUCTION TO MACHINE LEARNING

Machine Learning is defined as "learn from data. [64]" Machine learning uses many algorithms to learn the underlying pattern in the data and make the final decision. So, the data is very much essential to understand the patterns in the data. Data is defined as raw facts and figures, and machine learning algorithms utilize these facts and figures to generate the best information. Generally, datasets are the collection of rows and columns. Rows represent the examples in the datasets, also known as instances, whereas column represents the properties of the instances, also known as attributes or features. Attributes are either discrete and continuous. The discrete attribute has a finite set of values, whereas continuous attributes have infinite and absolute values. There are two types of data based on the availability of unique attributes. Data with a unique attribute is labeled, whereas a unique attribute or tag is unlabeled. The field of machine learning that deals with labeled data is known as supervised learning [65]. Furthermore, if the value of the unique attributes is numerical, e.g., predicting the height, the task called is regression, and if the value of a unique attribute is categorical, e.g., categorizing the grade of the students, the task is called classification task. Conversely, the field of machine learning dealing with unlabeled data is known as unsupervised learning. The field of machine learning that deals with unlabeled datasets are known as unsupervised learning. Generally, unsupervised learning aims to extract hidden functional patterns in the datasets. In Supervised learning, the labeled datasets are provided to the machine learning algorithm, and the goal is to generate a model that can learn the relationship

between input and output features. The model is provided with training data to generate accurate prediction by using an optimization algorithm, then generalizes the learning experience of the model to check the accuracy of output on new unseen data, also known as test data. The data is divided in three different sets, training, test and the validation set. The model is tuning on train set performance is improved by using the validation set, and test set are the unseen data utilized to check the model's performance. In unsupervised learning [66], the goal is to find the data's relationship and understand hidden patterns in the data. The task unsupervised of learning is divided into two subfields, i.e., Association learning and clustering. In association learning, the goal is to find the relationship between features of the training set. Clustering is another subfield of machine learning grouping of an item with similar properties are created. Items with similar properties are grouped in similar whereas another group is created for items with different properties. Figure 4.1. shows the general framework of machine learning.
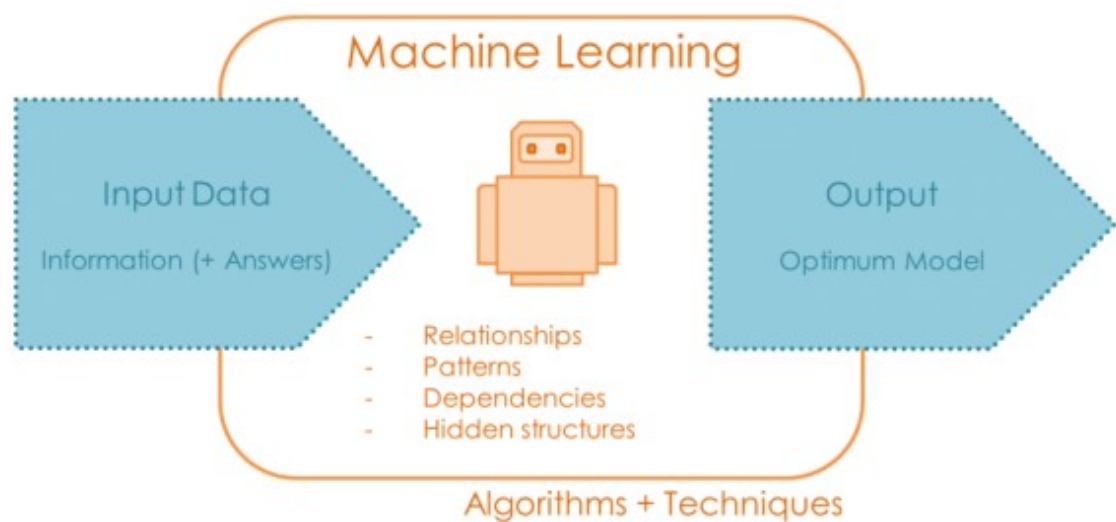
Figure 4.1: Machine Learning Framework

4.2 GENERALIZATION OF ML MODELS

Generalization in machine learning refers to how well the concepts learned from previously seen data by the machine learning model are applied to new unseen data [67]. The main goal of machine learning is to generalize well on any data to make the perfect prediction on any future problem. When we talked about generalization, two concepts are most familiar, namely, overfitting and underfitting. Underfitting and overfitting are

32

the most common problems everyone face for their machine learning model's poor performance. In overfitting, the machine learning model performs too well on training data. It is also defined as a complex model for simple data. Overfitting is solved by reducing the size of the data and using a straightforward model for uncomplicated data and a composite model for complex data. Underfitting occurs when the machine learning model could not understand the underlying pattern of the data. In underfitting, the machine learning model performs too poorly on training data. It is also defined as a simple model for complex data. The problem of underfitting is solved by increasing the size of the data. Figure 4.2. Illustrate the difference between the overfitting, underfitting, and best-fit machine learning model.
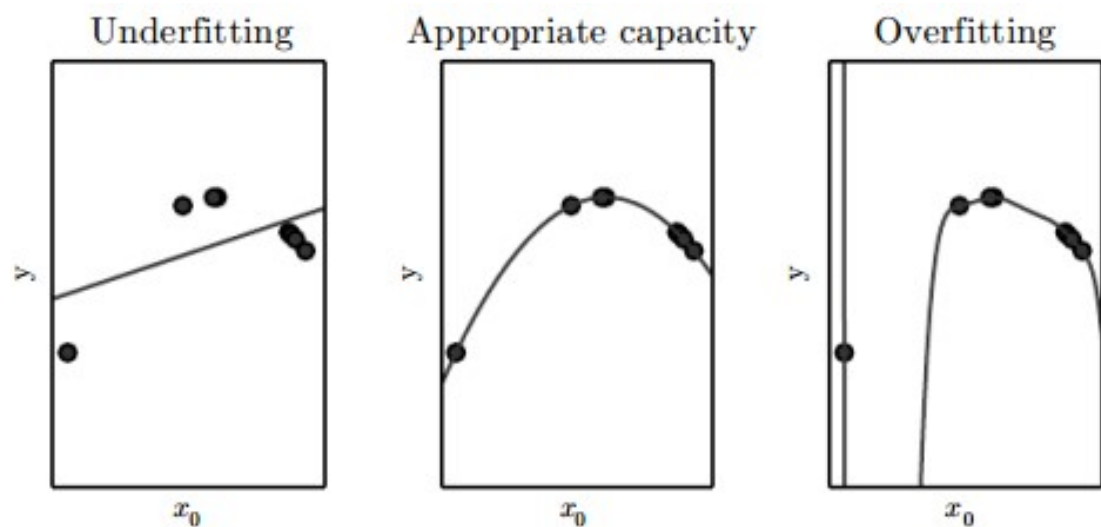
Figure 4.2: Comparison of Overfitting and Underfitting [68]

Machine learning algorithms can be divided into two general algorithmic categories i.e. linear and non-linear algorithms [69].

4.3   LINEAR ALGORITHMS

The linear algorithm assumes linear function as a prediction function for separating a set of features. A linear function consists of a finite number of features x1, x2,.,.,., xi then the linear function is represented as w0+ni=1wi*xi where w1, w2, wi are respective weights. If a prediction function is linear, then it can be used to perform prediction and regression tasks. In Figure 4.3(a), it is easy to draw a simple line to differentiate among

the data classes. So, using a linear classifier, it can be easily solved, whereas in Figure 4.3(b),
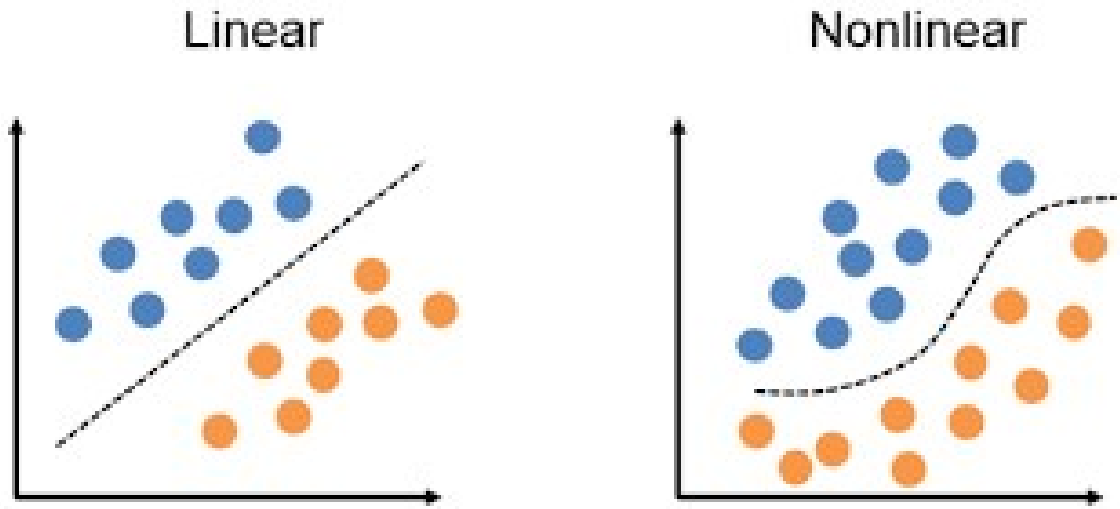
Figure 4.3: Data separation by linear Data non-linear separation model

it cannot be easy to draw a line to separate the classes so that a linear classifier will not work. Some of the prominent linear machine learning algorithms are mentioned below;

Linear regression is the most prominent and straightforward linear model that take for granted a linear relationship among a variable (y) which depends upon an independent variable (x) [70]. In a situation where there is a single independent variable, x1, that algorithm is known as simple linear regression. In contrast, if there are more independent variables such as (x1, x2,.,.,., xi), then the algorithm is known as multiple linear regression. Equation 1. represent the simple linear regression. Equation 2. Represent the multiple linear regression y = w0 + w1 × x y = w0 + w1 × x1 + w2 × x2 Logistic regression is another famous and standard linear machine learning algorithm [71]. As the name suggests, the logistic function is the core of the logistic regression algorithm. The logistic function is represented in equation 3.

Where e is the natural logarithm and t is a linear function.

4.4 NON-LINEAR ALGORITHMS

Linear models are unable to be performed on non-linear separated data. For that, non-linear come into play. Non-linear algorithms assume a non-linear function prediction function from making the decision. There are a number of non-linear machine learning algorithms available for solving classification problems. We will select the most are going to use the most of the mark machine learning algorithms to solve the problems regarding machine learning and classification, described below:

4.4.1 *K-Nearest Neighbor Classifier*

KNN is the noteworthy and explicit algorithm used in machine learning, usually employed for solving supervised learning problems. The distance among the test point with every point in the preparation data is calculated in this algorithm, afterwards at that point tracks down the k closest neighbor for that preparation point [72]. After feeding the test data into the model, the algorithm calculates the distance from every other point in the training data. Then it finds the nearest K members for that point. The K also helps us to classify the data into a particular group. The value of K gives us the number of nearest neighbors to consider while classifying the new data point.Figure 4.4 is the representation of KKN.
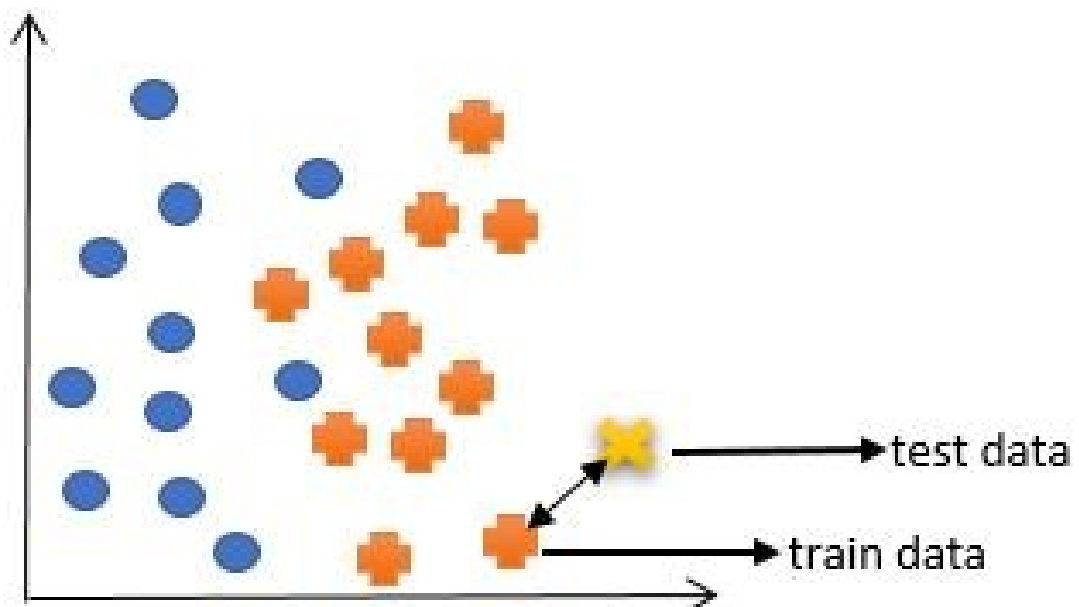
Figure 4.4: KNN representation

We can find the distance between two points by using the Euclidean distance formula.

Advantages

- It is simple to implement

- Makes no prior assumption of the data

Disadvantages

- As the model finds the distance between every point, its prediction time is high.

4.4.2 *Naive Bayes Classifier*

Naive Bayes is another generally noticeable, straightforward, and broadly utilized ML algorithm for settling classification problem. Conditional probability is involved in this algorithm. likelihood to order the test information into predefined classes. Conditional likelihood is the likelihood that defines if something will happen relies upon conditions. let us consider two events, M and N, and then the conditional probability is defined as P (M and N) = P(M)*P (N|M) Naive Bayes classifier locates each element's likelihood and then selects the component with the highest likelihood. The naive Bayes classifier is based on the Bayes rule. Bayes's rule helps us know how often A happens given that N already happens P(M|N) when we know that how often N happens given that A already happens P(N|M). Naïve Bayes Classifier finds the probability of every feature, and then it selects the outcomes with the highest probability.

Advantages

- Also, work on the small amount of data

- Easy and quick to predict the class of test data

Disadvantages

- Not suitable for large data sets

- Not work if features are correlated

4.4.3 *Decision Tree Classifier*

Decision tree is a well-known algorithm, used for the supervised learning problems such as regression and classification. This algorithm uses the mechanism of classification for prediction, assumes that every anticipation belongs to the most repeatedly occur ed class of training perceptions, in the zone where it belongs to [73]. The most often occurred class of training observations is taken as a reference and predict that every observation is associated with it in the zone where it belongs. The basic representation of decision tree is shown in Figure 4.5.
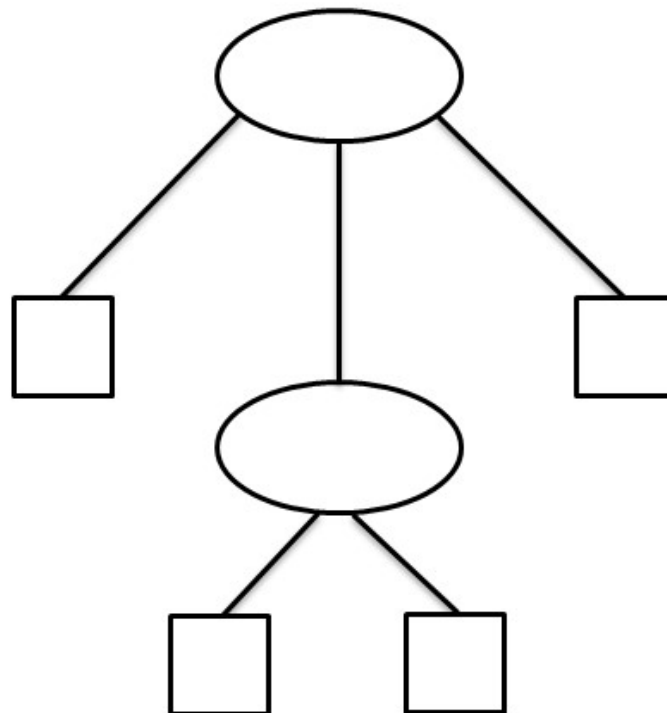

Figure 4.5: Representation of simple Decision Tree

Advantages

- Easy to understood and interpret

- Also, work on simple data

Disadvantages

- Likely to overfit

- It can be unstable for large datasets

4.4.4 *Random Forest*

Random Forest is the modern variation of the decision tree developed to solve the greedy problem of decision trees, and it is one of the most powerful and vital machine learning algorithms [74]. It can also be used to perform both classification and regression tasks by using ensembles of decision trees. Specifically, Random Forest creates multiple decision trees and merges them to get better accuracy in prediction. In contrast to the decision tree, which looks for the best split of input spaces, a Random Forest change this procedure to search the random samples of the features. The number of features that can be searched at each split point (m) can be specified as several algorithm parameters. For the classification task, the split point is defined as; m = p, while for regression, the split point is defined as; m = p3.

4.4.5 *Deep Learning*
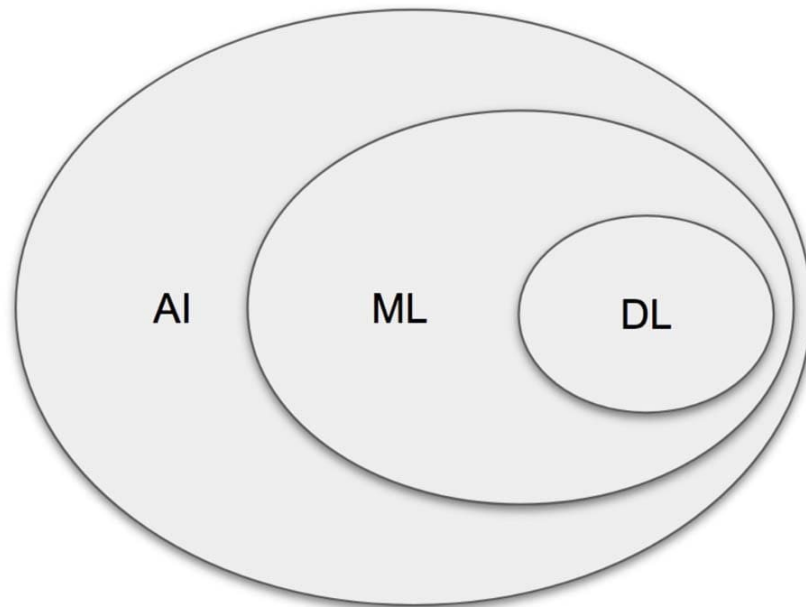
Figure 4.6: Difference among AI, ML, and DL

When we talk about deep learning, the first thing that came to mind is the difference or relationship between artificial intelligence, deep learning, and machine learning. So, before going to the details, let us understand the difference between them as illustrated in Figure 4.6. Artificial intelligence is "the science and engineering" of making intelligent machines, defined by John McCarthy, . It is the intelligence exhibit by the machine.

Arthur Samuel says: "When machines are given the ability to learn via explicit programming, this is machine learning. Similarly, Tom Mitchell defined machine learning as "A computer program is said to learn from experience E with respect to some task T and some performance measure P, if its performance on T, as measured by P, improves with experience E." Before defining deep learning, first, we need to understand neural networks. Neural Networks is the network of neurons or nodes connected and performed to receive input, do some computation and produce output. So, Deep learning is a specific sub-field of machine learning that emphasizes learning successive layers where meaning increases concerning the representation of layers. Artificial intelligence, deep learning and machine learning are related to each other. Its a hierarchy like machine learning has a sub-domain which is deep learning and machine learning itself is a sub-domain of Artificial intelligence which is the more general field of science and engineering.
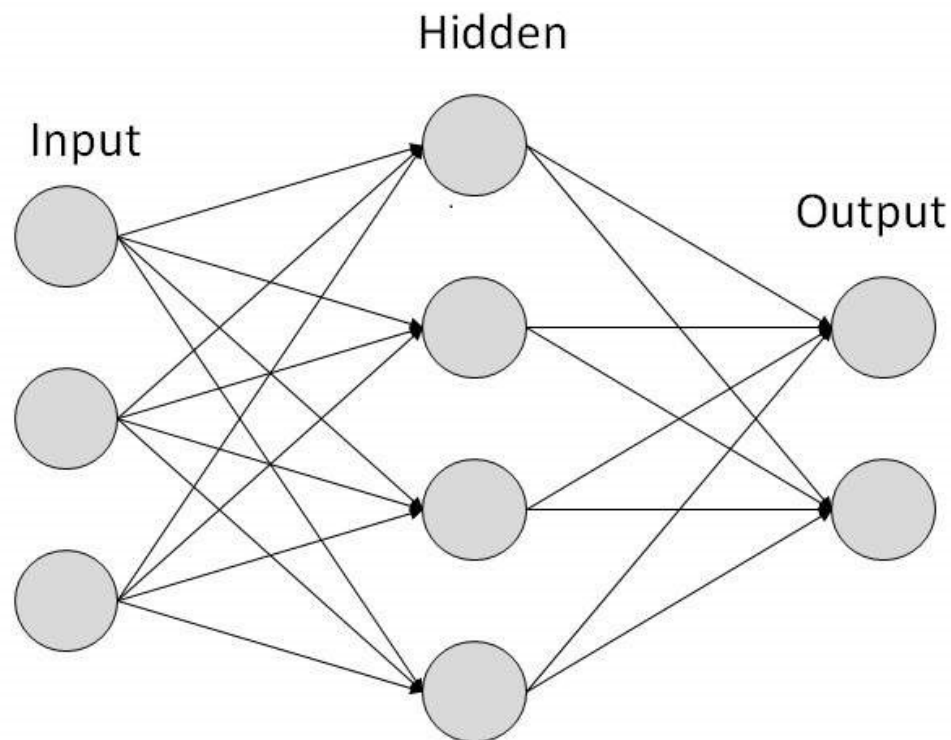
Figure 4.7: Neural network with only one hidden layer

Deep learning is the study of neural networks [75]. Deep in deep learning refers to the study of a successive or hidden layer of representations. The approach of machine learning that deals with the study of only one or two hidden layers are called an external network. Similarly, the approach of machine learning that deals with more than one or two layers is referred to as the deep neural network.

Artificial Neural Network The model, Artificial Neural Network (ANN) [76] stimulates the human brain. It is the network of layers that are connected to perform computation. The basic structure of ANN is made up of three central parts; known as input, hidden, and output layer. The simple ANN takes in some training data for train itself in-order to understand the pattern in that given data and use it to predict the output when some new data-set is provided. The input of any kind is provided in the input layer. The hidden layer is the core computational layer that performs all computation on the input. Each value is provided as input to each neuron in Layer 1. Neurons follow the neurons in previous layers in the successive layers via channels. Each channel is allocated some number, called weight. The values in the input layer are multiplied by the consistent weights, and their summation is provided as inputs to the neurons possessed by hidden layer, while each of these neurons is added with a constant number, known as 'bias'. The bias is then added to the input summation, then the obtained value is passed through a threshold function, known as activation function. The result of this activation function decides a binary decision for any neuron, to activate it or not . If a neuron is activated, it will send the data to the neuron of the following layer. In this manner, the data is transmitted across all the network, this process is the forward propagation. Then in the output layer, the highest values neuron fires and generates the probabilistic output, and this resultant value is called the predicted value. The predicted values are always different from the input value, and this difference is called an error, and there is a need to reduce the error. The given information is then moved back through the network, called Back-propagation. The weights are adjusted based on the information received from different cycles of forward and backward propagation until we receive an updated value of weight that minimize the difference between actual and predicted value.

4.5 CONVOLUTIONAL NEURAL NETWORK

Yann LeCun initiated the Convolutional Neural Network (CNN). This is a feed-forward ANN. Yann LeCun was a student of New York University in 1997. Inspired by the human visual cortex, the neuron of CNN followed a similar connectivity pattern. The visual cortex is the area of the brain cerebral cortex that is responsible for processing visual information. Visual input is providing from the eyes and reaches the visual cortex via the lateral geniculate nucleus in the thalamus. The state-of-the-art artificial
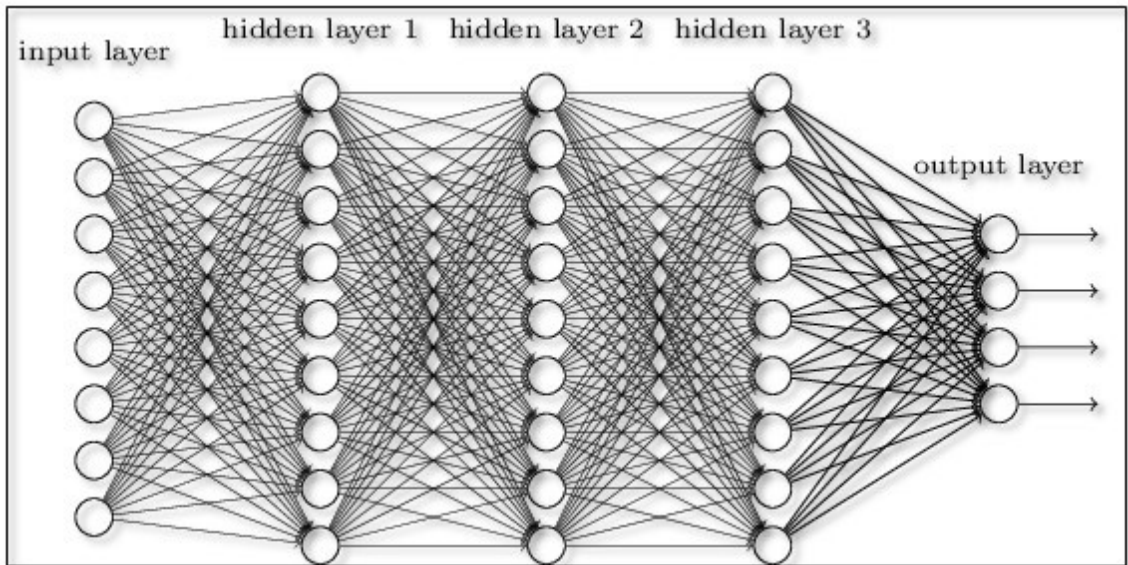
Figure 4.8: Neural network with more than one hidden layer

neural network is employed in many image processing and machine vision tasks such as image segmentation, image classification, and recognition. The standard CNN is composed of input layers, hidden layers, and output layers. The hidden layers are usually convolutional, pooling layers, and fully connected layers. The working of CNN is simple by comparing the pixels of the images. The pixels are also called features of the images. So, in short, CNN works by learning the features of the images, and CNN learns these features by passing through different hidden layers, and hidden layers in CNN are usually filters of different sizes.

4.5.1 *Convolutional Layer*
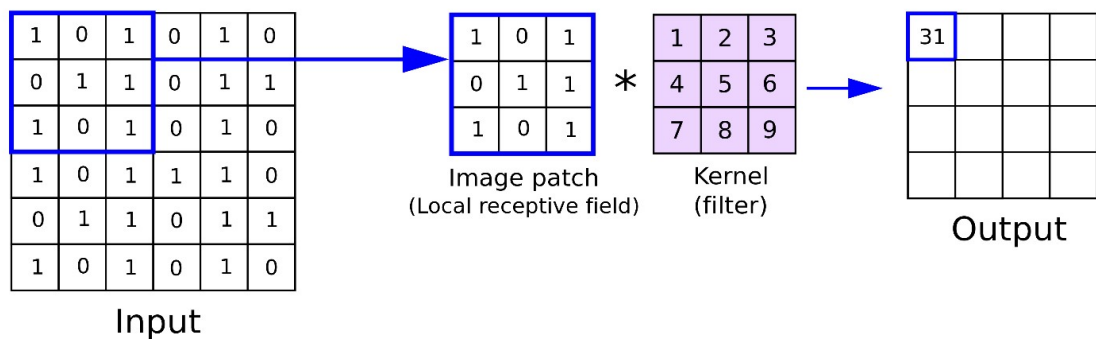
Figure 4.9: Example Convolutional Operation [77]

The convolutional layer is the main part of a convolutional neural network. It is the important layer responsible for feature extracting such edges and corners from the image. This layer is also responsible for identifying complex features such as shapes and digits. Convolution is a mathematical operation that takes an input image as a matrix and applies a filter or kernel that is also a matrix and generates the final image. Consider an input image of size (h x w x d) where h, w, and d are the input image's height, width, and dimension, respectively. Similarly, a filter of size (fh, fw, and fd) where fh, fw, and fd are the height, width, and dimension of the image of the filter. Then convolution operation generates the output of volume (h − fh + 1) x (h − fw + 1) x1. The example of convolution operation is shown in Figure 4.9.

4.5.2 *Padding*

The image size is shrinking after each convolutional layer which might result in the loss of valuable information. The solution to this problem is adding some extra layers to the border of the input image. There are two ways to pad an image. Adding zeros to the image's border so that the input and output image dimension is the same called 'same padding.' (n x n) * (f x f) = (n − f + 1) x (n − f + 1) On the other hand, 'valid padding' suggests no padding at all. The input image is left with its original shape. The equation is represented below, where 'p' is the number of layers to be added. (n + 2p) x (n + 2p) * (f x f) = (n x n) image. The Figure 4.10. Shows the padding of 1 layer to the input image

6x6 image

6x6 image with 1 layer of zero padding
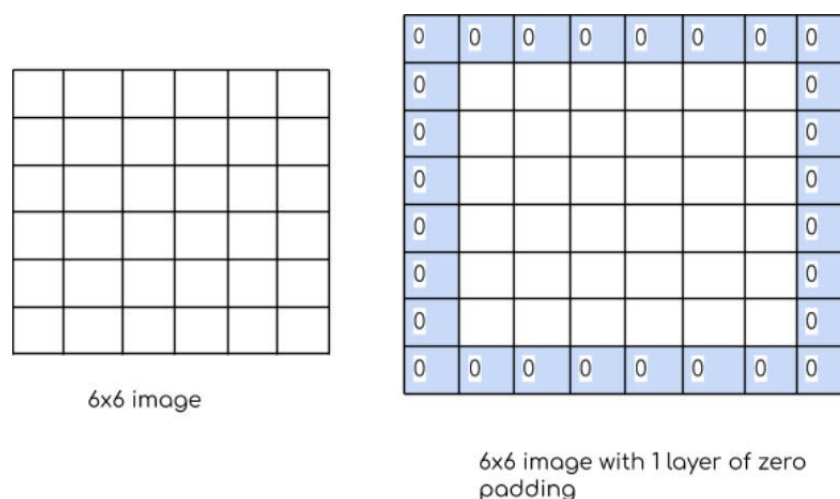
Figure 4.10: Zero paddings of 1 layer to an image of size 6x6 [78]

4.5.3   *Stride*

Stride is an essential parameter of CNN. It determines the moment of filter over the input image. Stride is usually set to be an integer value. For example, if the stride is equal to 1, then the filter will move 1 step at a time, below Figure 4.11. Clearly illustrate the concept of stride.
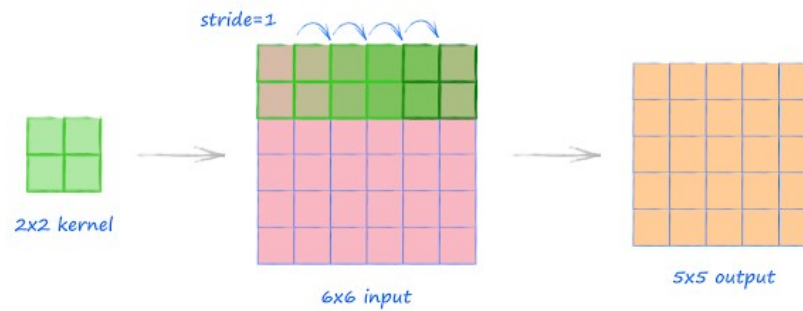
Figure 4.11: Working principle of stride [79]

4.5.4   *Pooling*

The pooling layer is also called the subsampling layer. Similar to the convolutional layer, the purpose of the pooling layer is the extracting features and reducing the size of the image. Two types of pooling techniques are often used: Max pooling and Average pooling. In max pooling, the maximum value from the pooling region is chosen. In Average pooling, the average of all values from the pooling region is taken.
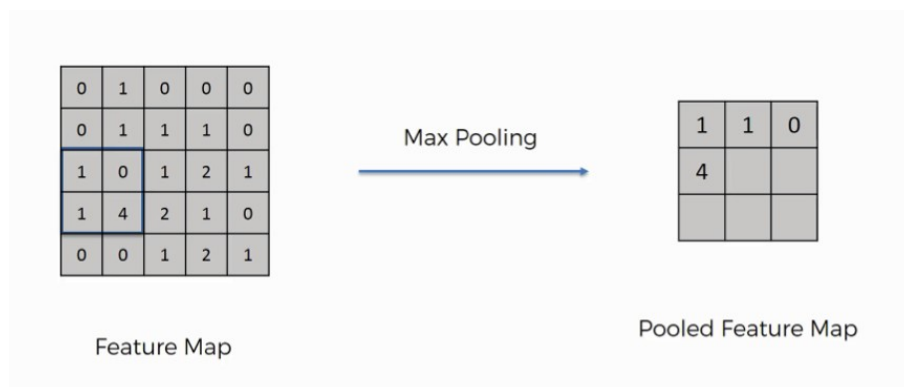
Figure 4.12: Max Pooling Example [80]

43

4.5.5 *Fully Connected Layer*

All the layers or techniques we discussed above are feature extracted techniques [81]. In a fully connected layer, we perform the actual classification of the output by flattening the image into a column vector. The flattened output is provided to the feed-forward neural network then Backpropagation is applied to every iteration. After the training series, the model can differentiate between dominating and low-level features and then perform classification by applying the SoftMax activation function. An example of the fully connected layer is shown in Figure 4.13.
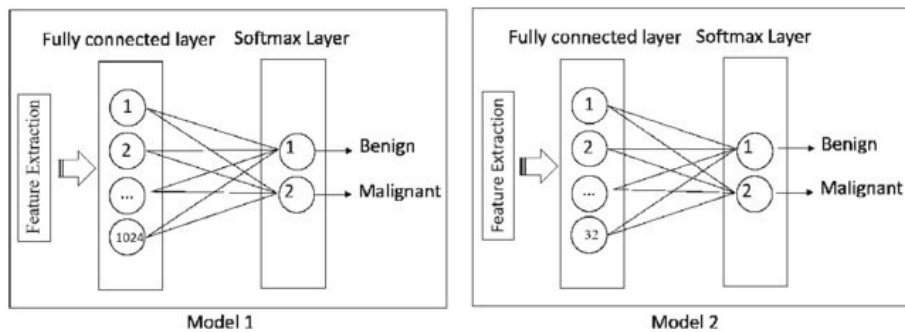
Figure 4.13: Fully connected SoftMax layer

4.5.6 *ReLU*

ReLU is the acronym of Rectified Linear Unit. It is the most prominent non-linear operation used in CNN. The output produced by the CNN till now is linear, so, the activation function precisely, a ReLU is applied to transform the linear value into a non-linear value. Out of other activation functions such as sigmoid or tanh, ReLU handles the vanishing gradient problem efficiently. The equation of the ReLU activation function is represented in equation (2).

f(x) = max (0, x)

4.5.7 *Backpropagation*

Backpropagation, short for 'Backward Propagation of error,' is a flexible and straightforward supervised learning algorithm for fine-tuning neural network weights. As the goal of all neural network is to reduce the difference between actual and predicted values Backpropagation help us to do so. We can do so by adequately tuning weights, making

the model reliable by increasing its generalization and reducing the error rate. The working of Backpropagation follows a six-step process.

- Input is provided to the artificial neural network

- Randomly initialized weights model input for each neuron

- Calculate the output of each neuron by summing the multiplication of each previous neuron

- Calculate the difference between the actual and expected value, i.e., error

  Error = Actual Output – Expected/Predicted Output

- Traverse back from the output to the hidden layer and adjust weights accordingly so that error is decreased

- Repeat the training until the difference between the actual and predicted value is minimized

Figure 4.14: Backpropagation workflow [82]

The grammatical representation of the backpropagation algorithm is shown in Figure 4.14.

4.6   CASE STUDY: ALEXNET

AlexNet was proposed by Alex Krizhevsky et al. [83] in 2012 and won the ImageNet large-scale visual recognition challenge (ILSVRC). It was the first CNN that utilizes the

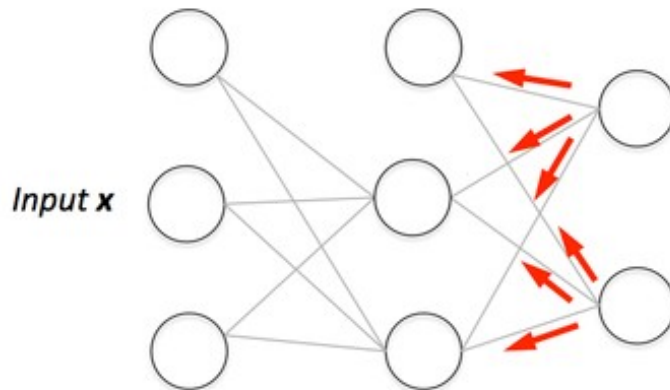power of GPU to increase performance. The AlexNet consists of eight layers, out of which five layers are convolution layers followed by three fully connected layers. Except for the output layer, the model uses ReLU as an activation function, and it was observed that using ReLU as activation boosts the training process by six times. The model also introduced padding to prevent the drastic reduction in the size of the feature map. The architecture of AlexNet is illustrated in Table I.

AlexNet starts with an image of (224x224x3) and uses 96 filters with size (11x11x3). A stride of 4 is applied and obtained resultant image of size (55x55x96). Then a max-pooling was applied to extract the features further. It is noted that each ReLU is applied in a convolutional layer. The second convolutional layer uses the image of size (27x27x96) and uses 256 filters with size (5x5x3), and a stride of 4 is applied and obtained resultant image of size (27x27x256). Then a max-pooling was applied to extract the features of size (13x13x256). Similarly, three more convolutional layers, one max-pooling, and three fully connected layers with different filter sizes were applied to extracted 4096 features and 62.3 million parameters. To perform classification, the final layer AlexNet is the 1000-way SoftMax function.

Layer		Feature Map	Size	Kernel Size	Stride	Activation
Input	Image	1	227x227x3	-	-	-
1	Convolution	96	55 x 55 x 96	11x11	4	relu
	Max Pooling	96	27 x 27 x 96	3x3	2	relu
2	Convolution	256	27 x 27 x 256	5x5	1	relu
	Max Pooling	256	13 x 13 x 256	3x3	2	relu
3	Convolution	384	13 x 13 x 384	3x3	1	relu
4	Convolution	384	13 x 13 x 384	3x3	1	relu
5	Convolution	256	13 x 13 x 256	3x3	1	relu
	Max Pooling	256	6 x 6 x 256	3x3	2	relu
6	FC	-	9216	-	-	relu
7	FC	-	4096	-	-	relu
8	FC	-	4096	-	-	relu
Output	FC	-	1000	-	-	Softmax

Figure 4.15: Summary of ALexNet [84]

To summarize,

- AlexNet is an 8-layer neural network comprised of 5 convolution layers with max-pooling, and 3 are fully connected layers.

46

- ReLU is the activation function applied to each convolution layer SoftMax is the activation function applied to the final layer

- The architecture also utilizes two Dropout layers

- A total of 62.3 million learning parameters are achieved in architecture

4.7 METHODOLOGY

4.7.1 *Proposed Framework of Segmentation of Brain Tumor*
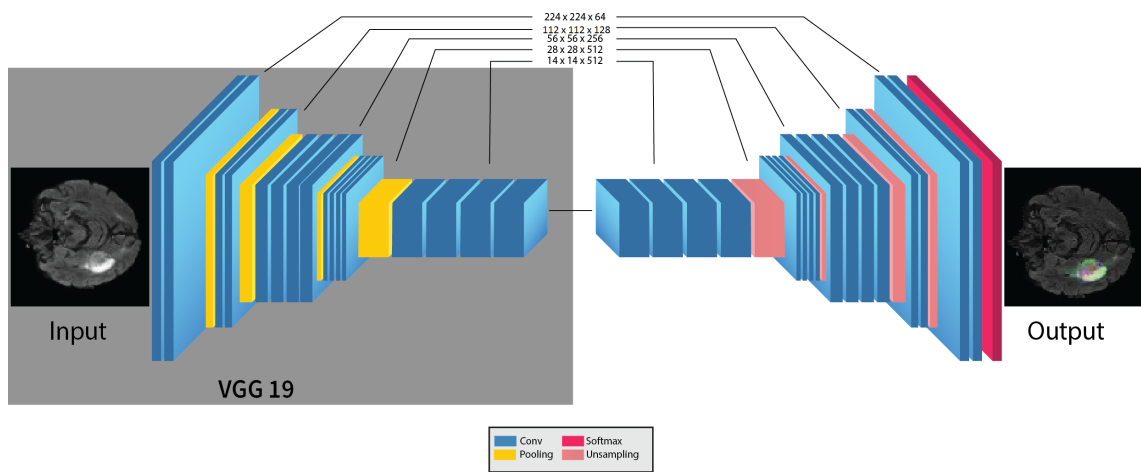
Figure 4.16: A framework of Segmentation of Brain Tumor

The framework of Segmentation of Brain Tumor is shown in Fig 4.16. Similar to the standard UNET [85], the proposed framework comprises of encoder and decoder part. The encoder part is standard VGG19 [86] used to extract features from MR images; meanwhile, the decoder part uses the output of encoder VGG19 to segment the image by upsampling the feature maps. The figure also shows that different hidden layers are represented by different colors. The convolutional layers are represented by blue color, yellow are pooling layers, upsampling layers are represented by pink color and finally the SoftMax layer is represented in red color. Input is provided at encoder part and after passing through different hidden layer output segmented image is received at the end of decoder part. Initially there are 114 million parameters of VGG19 that is reduced to 36.1 Million parameters by discarding Fully Connected layer layers. Output is passed to SoftMax layer to classify pixel independently into 'K' classes. Where 'K' is number of classes. In this K is equal to four because we have classes with (0,1,2,3) labels. 0 for

non tumorous, 1 for CT, 2 for WT and 3 for ET.

- Encoder

Figure 4.17: A framework of Segmentation of Brain Tumor

The architecture of Encoder is represented in Figure 4.17. The encoder network performs convolution with a filter to produce a set of feature maps. Then Rectified Linear Unit (ReLU) is applied to transform the non-linear output into linear output. Then the output is Batch normalized. Also, the Maxpooling layer with a 2×2 window and stride 2 is performed to reduce the dimension of the image. In this case we discard FC layer to reduce the parameters learns from 114 Million to 36.1 Million parameters.

- Decoder

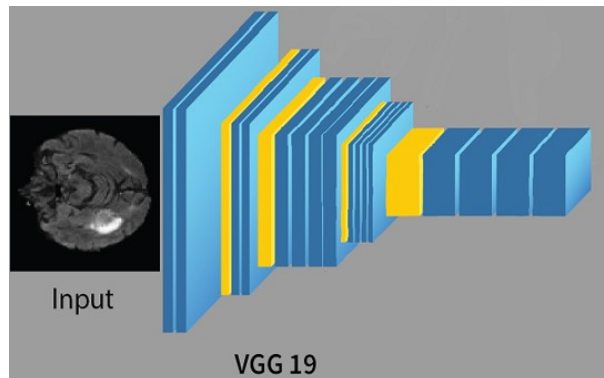**Figure 4.18:** A framework of Segmentation of Brain Tumor

The architecture of decoder is represented in Figure 4.18. The input feature map is up-sampled by the decoder network. The decoder which corresponds to the initial encoder (front to the image which was input), generates a feature map which is multi-channel. The next process is the representation of the high dimensional

48

feature at the output of the last decoder, it is fed to a softMax classifier, which is trainable and its output is a 'K' channel image of probabilities, where 'K' represents the number of classes.

4.7.2 *Datasets*

For the evaluation of proposed frameworks, two types of datasets were used. Specifically, for the segmentation task, the BRATS20 [26] was used, consisting of 371 image files, and each file is composed of five subfiles, out of which four files are MRI modalities of the individual patients one file is the target mask of the individual patient. T1, T2, T2*, and Attenuated Inversion Recovery (FLAIR) weighted mages are the most common modalities of MRI utilizes in this dataset. Each modality was acquired different clinical protocol and multiple scanners from a number of institutions and each modality have been segmented manually by one to four raters. All the modalities are available as NIFTI file with the extension of (.nii.gz). NIFTI file is the most common file format for neuroimaging.

Similarly, for survival prediction, BRATS20 survival info was used. The datasets are composed of 371 entities of the individual patient, which are the pseudo identifier of the imaging data. The survival info datasets include patients' age and resurrection status of the patients.

4.7.3 *VGG19*

VGG19 is the commonly used CNN composed of 19 layers. Out of 19 layers, 16 are convolutional layers, five max-pool layers, the three completely connected layers, and 1 SoftMax layer. The architecture of VGG19 [86] is simple that follows the six steps process.

- First, the image is provided as input to the architecture; usually, the shape (224, 224, 3) is provided as input.

- Then, the kernel of size (3, 3) was applied to discover the underlying patterns of the image.

- Padding was used to preserve image resolution

- Pooling was applied to reduce the dimension of the image

- The output of the layers is usually linear. Therefore, a fully connected layer was applied to transform the linear output into the non-linear output

- Finally, the SoftMax layer is applied to predict the probability distribution of the multiple classes

The training of VGG19 from scratch is a tedious and complex task; therefore, nowadays, a pre-trained VGG19 is often used. A pre-trained VGG19 is usually trained on larger datasets, i.e., ImageNet therefore, the learning of new and complex patterns becomes efficient and straightforward.

Figure 4.19: VGG19 Architecture

4.7.4 *UNET*

Image segmentation refers to partitioning an image into distinct regions or categories, with each region contains pixels with similar attributes, and each pixel in an image is allocated to one of these categories. UNET is the state-of-the-art variant of convolutional neural network widely used for medical image segmentation. UNET was initially proposed by Olag Ronneberger et al. [85] in 2015. The simple UNET comprises two paths: contracting path (encoder) and expansive path (decoder). The general CNN's encoder part consists of the input layer, convolutional layer, pooling layer, and fully connected layer. It is used to extract features from the images, and each downsampling doubles the number of features. The decoder part uses transposed convolution to permit localization. It consists of upsampling of the feature map, which helves the number of feature channels. The concatenation of corresponding feature maps of encoder and decoder is also performed, and finally, a convolutional layer was applied to map the channels to the corresponding classes.
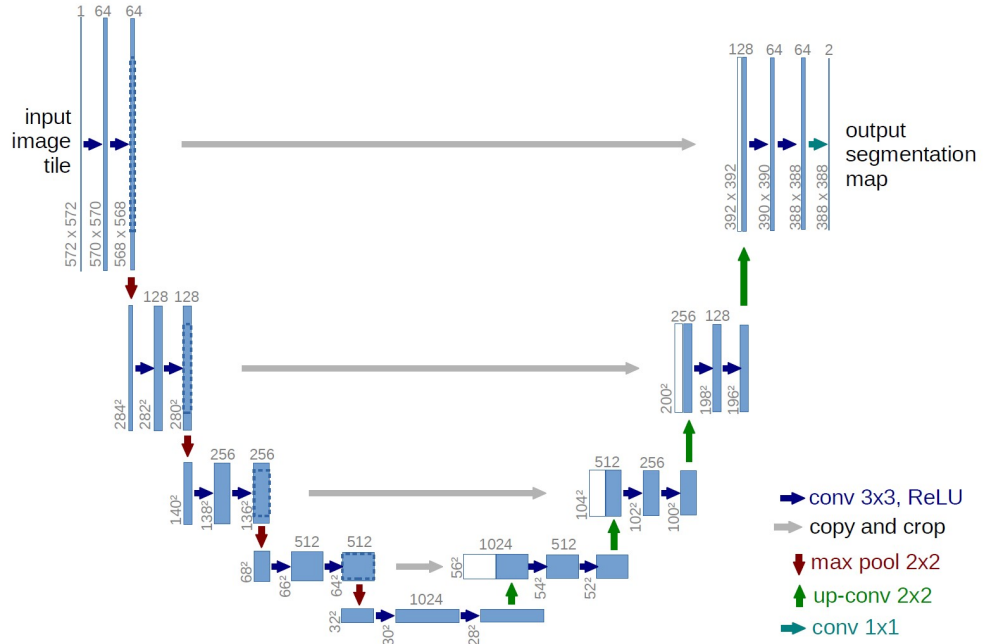
Figure 4.20: UNET Architecture

4.7.5 *Feature Extraction*

The overall survival info datasets consist of 371 entities having four columns i.e. age of the patient, Pseudo identifier of image, survival days and Gross Total Resection (GTR). The output of segmentation task serve as an input to survival prediction task because segmented image contain useful feature like volume of enhancing tumor, whole tumor and core tumor therefore in this case volume of edema, necrotic, and enhancing tumor along with age of the patient are taken as feature and utilizes for the survival prediction task. From survival days we assign the labels to the features by using the intuition if Survival Days is less than 250 then the category 'Short' is assign, else if Survival days is greater than 250 and less than or equal to 450 then category Medium is assign and everything else is assign in the Long category.

Table 4.1: Feature Extracted for overall Survival Prediction

S. No.	Age	ET	WT	TC
1.	57.000	0.015202	0.039171	0.019636
2.	83.649	0.039530	0.048636	0.025146
3.	60.019	0.000448	0.018200	0.071834

The framework of the survival prediction task is shown in Figure 4.19. Each part of the framework is discussed below.
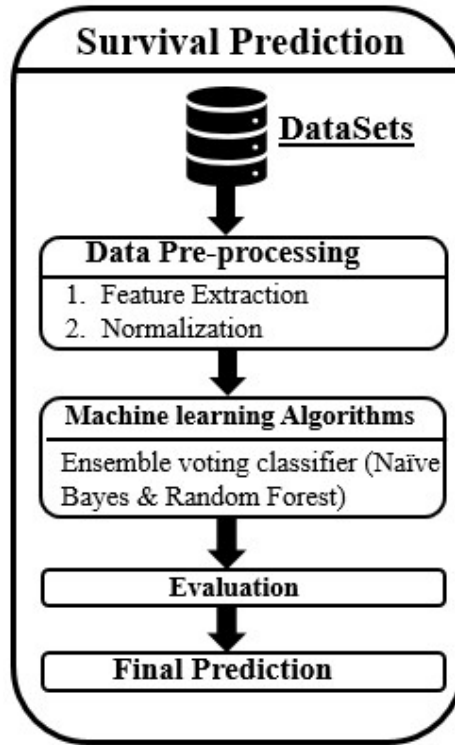
Figure 4.21: A framework of Survival Prediction

4.7.6 *Normalization*

All four columns of the datasets contain values ranges from positive infinity to negative infinity. In this case, it difficult for the learning algorithm to find the hidden pattern in the datasets; therefore, in this paper, we use Minmax normalization to limit the values between 0 and 1 [88]. It can easily be performed by using the MinMaxScaler() function of Scikit Learn preprocessing in python. Minmax normalization preserves the linear transformation of the attributes. The equation for Minmax normalization is represented in equation (1). The equation shows that mini is the minimum value of the attribute and maxi is the maximum value of the attribute and vi is the attribute value whose normalization is performed, and vi is the final normalized value.
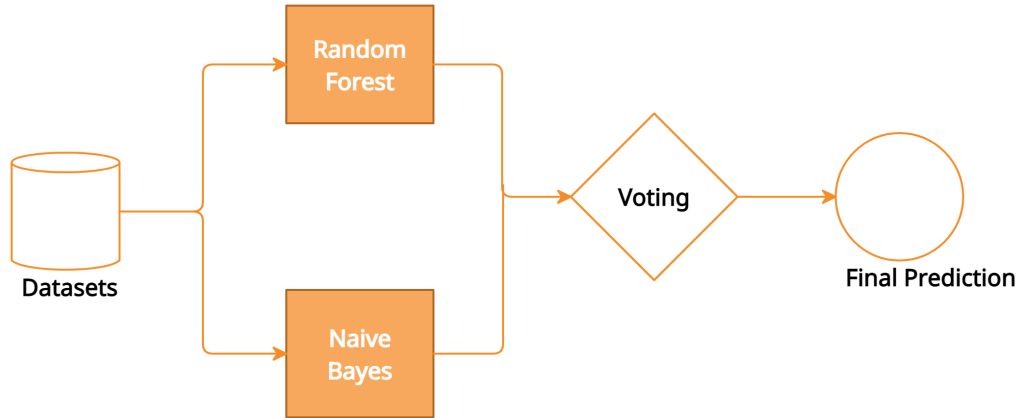
Figure 4.22: Overview of Ensemble Voting Classifier

4.7.7 *Ensemble Classifier*

The Figure 4.20. represent the flow of overall patient survival prediction framework. Ensemble learning is a machine learning technique that combines multiple machine learning models to produce optimal prediction results. To further improve prediction performance, an ensemble of random forest Naïve Bayes (NB) is performed by applying a hard voting classifier that means we predict class labels by majority rule voting instead of probability-based. Random forest is a prominent ensemble model that is the combination of multiple decision trees. A decision tree is the most powerful and essential algorithm for predictive modeling machine learning. The decision tree is known by its modern name Classification and Regression Tree (CART) [89]. Therefore, it can be used to resolve the problems of regression and classification. The decision tree can perform classification by sorting down the training data from the top (root) node to the tree's bottom (leaf) node. Each instance is classified by starting from the tree's root node, then testing the instance specified by the node and moving down to the leaf node. This process is repeated for all subtrees rooted at the new nodes. Meanwhile, NB is another supervised machine learning algorithm use to classify data into predefined classes. It simply did this by finding the probability that something will happen, given that something else has already happened. Therefore, this task ensemble, voting classifier of random forest, and NB were applied to classify the patient survival into short, medium, and long survival classes. We also set the voting = 'hard' which means we assigned the majority rule voting for classification instead of probability based

Chapter Summary

In this chapter, a broad overview of machine learning principles and generalization of machine learning models are discussed. Then, the most prominent and highly useful machine learning models are described in details. Furthermore, a complete background and working of convolutional neural network is discussed and finally, the working of proposed methodologies for segmentation of brain tumor and overall survival prediction is given.

Experimental Evaluation

In this section, evaluation metrics and obtained results are described in detail.

5.1 EVALUATION METRICS

Generally, there two types of Segmentation of Brain Tumor used, i.e., manual segmentation and automatic segmentation. Firstly, the manual segmentation is performed by MRI experts that are tedious and complex tasks, but accurate, while the accurate and straightforward software does automatic segmentation due to development in artificial intelligence. It is also worth mentioning that the MRI experts first label the datasets used for automatic segmentation. The evaluation metrics use for Segmentation of Brain Tumor are DSC, accuracy, sensitivity, and precision. Meanwhile, the evaluation metric for brain tumor survival prediction are the accuracy of the prediction. TP refers to tuple to the positive tuple that is accurately labeled by the classifier [90]. Similarly, TN refers to the negative tuple that is correctly labeled by the classifier. FN refers to tuple to the positive tuple that is incorrectly labeled by the classifier. Similarly, FP refers to the negative tuple that is incorrectly labeled by the classifier.

Dice coefficient Score (DSC) is the commonly used evaluation metric for image segmentation and Segmentation of Brain Tumor. DSC is the measure of overlapping area between two images [91]. For example, in Figure 5.1. There are two circle images of the name image 'A' and image 'B.' Then the DSC of the figure is illustrated in equation (1) that shows that DSC is equal to two times of overlap area into the overall area of picture element of both images. It can also be

illustrated as the two times of TP divided by total TP, FP and FN represented in equation (2). DSC = 2 |AB| / (|A|+|B|)
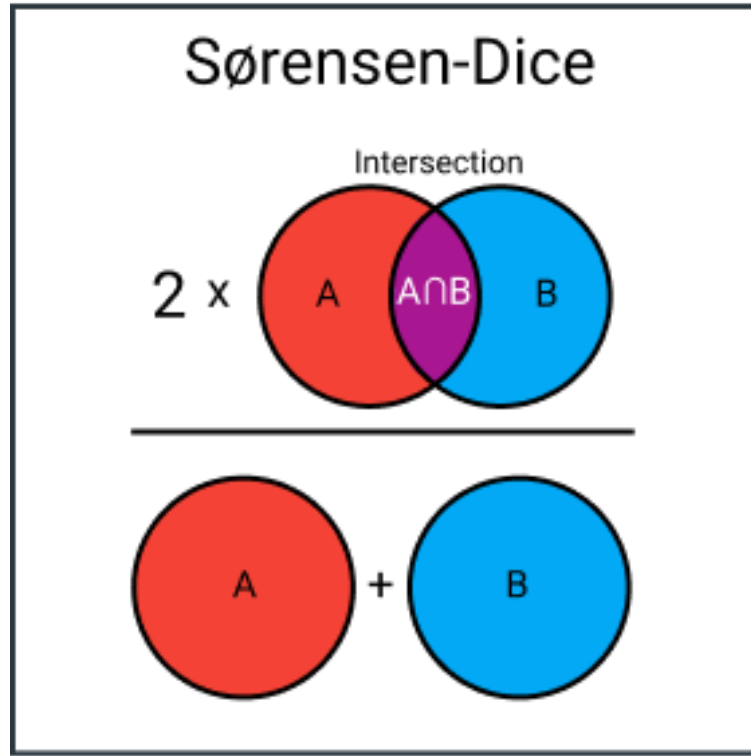
Figure 5.1: Dice Coefficient Example

$$DSC = \frac{2TP}{2TP + FN + FP} \tag{5.1.1}$$

Sensitivity is the ratio of TP to TP and FN, as illustrated in equation (1).

$$Sensitivity = \frac{TP}{TP + FN} \tag{5.1.2}$$

Specificity Specificity is the ratio of TN to TN and FP illustrated in equation (4).

$$Specificity = \frac{TN}{TN + FP} \tag{5.1.3}$$

Precision is the ratio of TP to TP and FP illustrated in equation (5).

$$Precision = \frac{TP}{TP + FP} \tag{5.1.4}$$

Recall is the ratio TP to TP and FN illustrated in equation (8).

$$Accuracy = \frac{TP + TP}{FN} \tag{5.1.5}$$

Accuracy is the ratio of TP and TN to total positive (P) and negative (N) illustrated (9).

$$Accuracy = \frac{TP + TN}{P + N} \qquad (5.1.6)$$

Intersection Over Union (IOU) is the another prominent used evaluation criteria in image segmentation. It is defined as the ratio of the intersection region of images to the union of two images. The equation (10) represents the equation of IOU.

$$IOU = \frac{TP}{FP + TP + FN} \qquad (5.1.7)$$

5.2 DATASETS

For the evaluation of proposed frameworks, two types of datasets were used. Specifically, for the segmentation task, the BRATS20 [87] was used, consisting of 371 image files, and each file is composed of five subfiles, out of which four files are MRI modalities of the individual patients one file is the target mask of the individual patient. T1, T2, T2*, and Attenuated Inversion Recovery (FLAIR) weighted mages are the most common modalities of MRI utilizes in this dataset. Similarly, for survival prediction, BRATS20 survival info was used. The datasets are composed of 371 entities of an individual patient, a pseudo identifier of the imaging data. The survival info datasets include patient's age and resurrection status of patients. The Figure 5.2. Represents the MRI modalities with the ground mask.
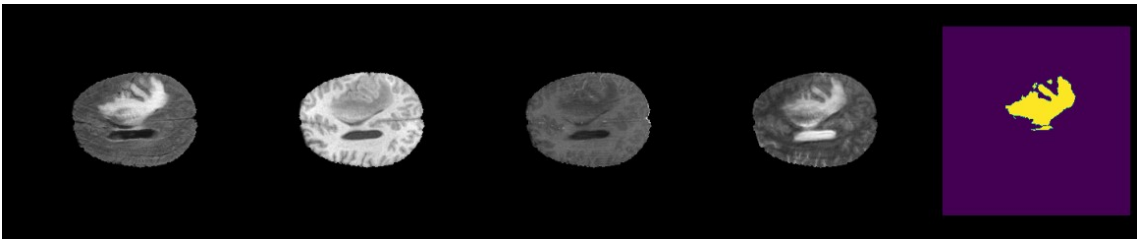
Figure 5.2: MRI modalities and ground mask

5.3 QUANTITATIVE EVALUATION

In this section, a comparison of both proposed methods are performed, respectively. The results demonstrate that the performance of VGG-UNET is better for ET and TC as

compared to the previous method. Similarly, the performance of the proposed Ensemble Voting Classifier is better than previous methods.

Table 5.1: Comparison of Segmentation of Brain Tumor Results

S. No.	Methods	ET	WT	TC
1.	Ghaffari et al. [91]	0.78	0.90	0.82
2.	Ballester et al. [92]	0.67	0.85	0.78
3.	Colman et al. [93]	0.75	0.86	0.79
4.	Proposed Method	0.81	0.88	0.86

5.4 QUALITATIVE EVALUATION

5.4.1 *Results of VGG19 Encoder UNET*
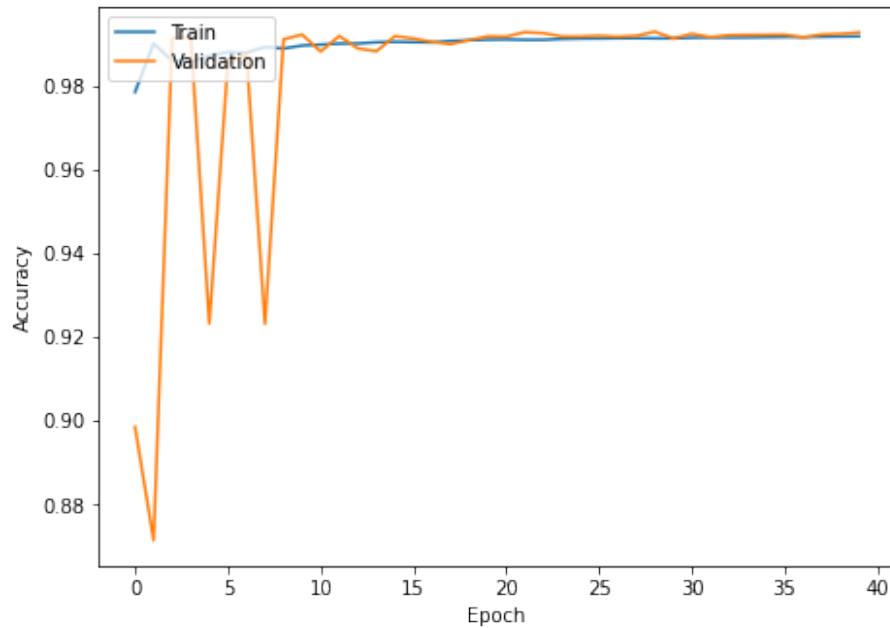
Figure 5.3: Comparison of Accuracy w.r.t number of epochs

The Figure 5.5. shows the accuracy curve that is the most important curve to understand the progress of machine learning algorithms. The curve illustrate that initially the train accuracy is 90% and decreases in first 2 epochs and begin to increase from second epoch and with the number of 40 epoch train accuracy is approach to 99.7%. The test accuracy

begins from 98% and with increases in the number of epoch test accuracy approaches to 99%.
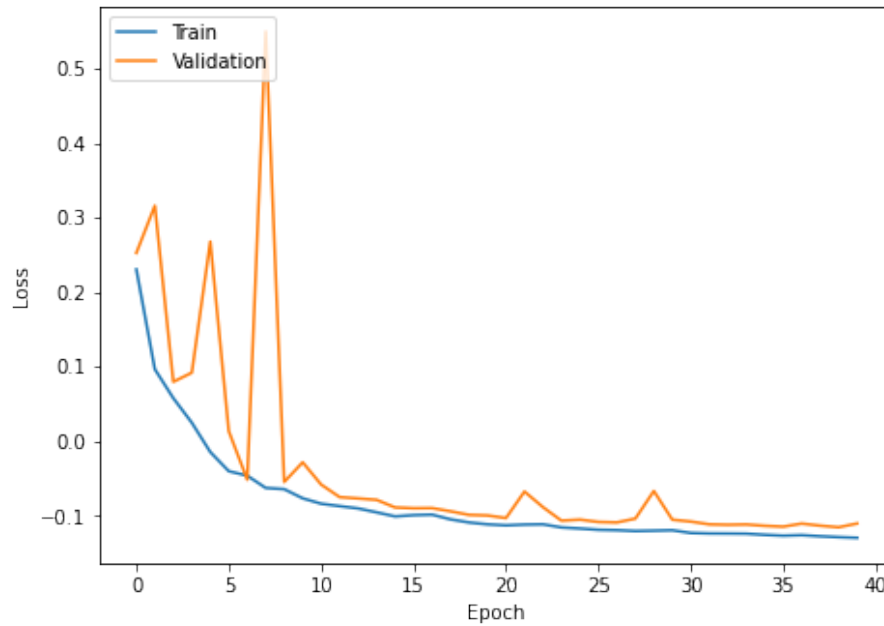
Figure 5.4: Dice coefficient loss w.r.t number of epochs

The Figure 5.6. represents another important curve that is the loss curve and is the curve between Loss and number of epochs. The curve illustrate that train loss consistently decreases with increasing in the number of epochs. Similarly, the train loss also decreases with increases in the number of epochs but train loss decreasing is inconsistent.

Table 5.2. illustrate the segmentation results

Table 5.2: Results of Segmentation

S. No.	Metrices	Results
1.	Sensitivity	0.997
2.	Specificity	0.991
3.	Precision	0.925
4.	Accuracy	0.994
5.	Dice Coefficient of ET	0.8189
5.	Dice Coefficient of WT	0.8876
6.	Dice Coefficient of TC	0.8648

5.4.2 *Results of Ensemble Model*

Table 5.3: Results of Brain Survival Prediction

S. No.	ML Algorithms	Accuracy
1.	KNN	54%
2.	Decision Tree	46%
3.	SVM	55%
4.	Ensemble Classifier	62.73%

The evaluation metrics used for brain tumor survival prediction are accurate, and comparison of the achieved prediction results with prominent machine learning algorithms are illustrated in Table 5.3.
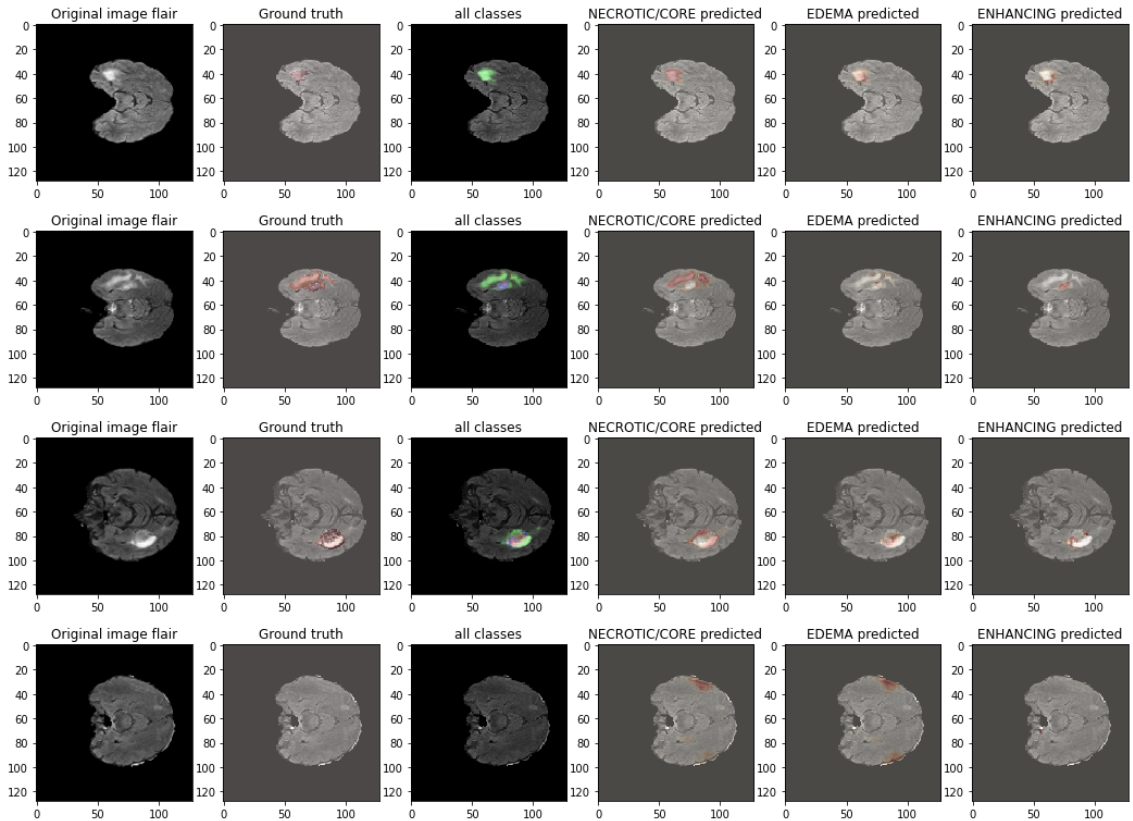
Figure 5.5: Generated Results

Similarly, the comparison of proposed ensemble voting classifier for overall survival prediction with other prominent techniques are illustrated in Table 5.4.

The qualitative results of the segmentation of brain tumor is shown in Figure 5.5. The

Table 5.4: Comparison of Overall Survival Prediction Results

S. No.	Method	Accuracy
1.	Agravat et al. [56]	56.8%
2.	Ali et al. [63]	57%
3.	Proposed Ensemble Voting Classifier	62.73%

first column of the image is the input image. The next column is the ground truth of the corresponding input image. Then, the third column represents the segmentation of all tumorous classes. The forth, fifth and sixth columns are individual segmentation of core, whole and enhancing tumor respectively.

Chapter Summary

In this chapter, a qualitative and quantitative results are presented. Additionally, an evaluation matrices used in the experimentation are also described along with the datasets. Furthermore, the evaluationn of achieved results with the previous methods are also presented.

CHAPTER 6

CONCLUSION & FUTURE WORK

6.1 CONCLUSION

To conclude a pretrained VGG19-UNET was trained for segmentation of Brain Tumor. The evaluation is carryout on BRATS20 and evaluation metrics use in the segmentation method are accuracy, sensitivity, specificity, precision and DSC. The obtained results shows that proposed model produces more accurate and better outputs than previous method for enhancing tumor and core tumor with dice coefficient score of 0.81 and 0.86 respectively. Furthermore, an ensemble model of random forest and Naïve Bayes was applied for patient's survival prediction and achieve prediction accuracy of 62.7%. The proposed segmentation methods enable the efficient and effective diagnosis of brain tumor whereas ensemble method enable the early survival prediction.

6.2 CONTRIBUTION

The contribution of proposed architectures is summarized as:

- Fully automated system for Segmentation of Brain Tumor and patient survival prediction

- Encoder decoder model for brain tumor segmentation and ensemble model for survival prediction

- An encoder part of the model is pretrained VGG19 followed by respective decoder part

- An ensemble voting classifier of Random Forest and Naïve Bayes for patient survival prediction

- Review and distinguish of proposed methods with previous prominent methods

6.3   FUTURE WORK

In this research, we used BRATS'20 to perform Detection of Brain Tumor and survival prediction. We achieved better DSC on segmentation of core and enhancing tumor however we are unable to increase DSC of whole tumor segmentation. Therefore, our future work will be focus on refining all tumor types. We can do so by using generative models. Furthermore, our proposed architecture is general so someone can be used it on different datasets for enhancing segmentation and prediction results.

References

[1] Agravat, Rupal R., and Mehul S. Raval. "Prediction of overall survival of brain tumor patients." In TENCON 2019-2019 IEEE Region 10 Conference (TENCON), pp. 31-35. IEEE, 2019.

[2] Menze, Bjoern H., Andras Jakab, Stefan Bauer, Jayashree Kalpathy-Cramer, Keyvan Farahani, Justin Kirby, Yuliya Burren et al. "The multimodal brain tumor image segmentation benchmark (BRATS)." IEEE transactions on medical imaging 34, no. 10 (2014): 1993-2024.

[3] Havaei, Mohammad, Axel Davy, David Warde-Farley, Antoine Biard, Aaron Courville, Yoshua Bengio, Chris Pal, Pierre-Marc Jodoin, and Hugo Larochelle. "Segmentation of Brain Tumor with deep neural networks." Medical image analysis 35 (2017): 18-31.

[4] Pereira, Sérgio, Adriano Pinto, Victor Alves, and Carlos A. Silva. "Segmentation of Brain Tumor using convolutional neural networks in MRI images." IEEE transactions on medical imaging 35, no. 5 (2016): 1240-1251.

[5] Minaee, Shervin, Yuri Y. Boykov, Fatih Porikli, Antonio J. Plaza, Nasser Kehtarnavaz, and Demetri Terzopoulos. "Image segmentation using deep learning: A survey." IEEE Transactions on Pattern Analysis and Machine Intelligence (2021).

[6] Tiwari, Arti, Shilpa Srivastava, and Millie Pant. "Segmentation of Brain Tumor and classification from magnetic resonance images: Review of selected methods from 2014 to 2019." Pattern Recognition Letters 131 (2020): 244-260.

[7] Esteva, Andre, Katherine Chou, Serena Yeung, Nikhil Naik, Ali Madani, Ali Mottaghi, Yun Liu, Eric Topol, Jeff Dean, and Richard Socher. "Deep learning-enabled medical computer vision." NPJ digital medicine 4, no. 1 (2021): 1-9.

[8] Omuro A, DeAngelis LM. Glioblastoma and Other Malignant Gliomas: A Clinical Review. JAMA. 2013;310(17):1842–1850. doi:10.1001/jama.2013.280319.

[9] Kalender, W. A. (2011). Computed tomography: fundamentals, system technology, image quality, applications. John Wiley Sons.

[10] HKH joshua. [online], https://hkhjoshua.wordpress.com/2014/10/17/new-post/, Last accessed on June, 2021

[11] Leighton, T. G. (2007). What is ultrasound? Progress in biophysics and molecular biology, 93(1-3), 3-83

[12] Radiology Key. [online], https://radiologykey.com/instrumentation-and-controls/, Last accessed on June, 2021

[13] Teach Me Anatomy, https://teachmeanatomy.info/the-basics/imaging/x-ray/, Last accessed on June, 2021

[14] Broadhouse K (2019) The Physics of MRI and How We Use It to Reveal the Mysteries of the Mind. Front. Young Minds. 7:23. doi: 10.3389/frym.2019.00023

[15] Chen, Bo. "Basics of Pulse NMR and Relaxation." (2020): 3-1.

[16] Relaxation. In: How Does MRI Work? Springer, Berlin, Heidelberg (2006). https://doi.org/10.1007/978-3-540-37845-7

[17] Weishaupt, Dominik, Victor D. Köchli, and Borut Marincek. How does MRI work? an introduction to the physics and function of magnetic resonance imaging. Springer Science Business Media, 2008

[18] Slice Selection and Spatial Encoding. In: How Does MRI Work? Springer (2006), Berlin, Heidelberg. https://doi.org/10.1007/978-3-540-37845-7_4

[19] Han, Yoseo, Leonard Sunwoo, and Jong Chul Ye. "k-Space Deep Learning for Accelerated MRI." IEEE transactions on medical imaging 39, no. 2 (2019): 377-386

[20] Magnetic Resonance Imaging (MRI) of the Brain and Spine. [online], https://case.edu/med/neurology/NR/MRI%20Basics.htm, Last accessed June, 2021

[21] Structure and Function of Human Brain. [online], https://www.nbia.ca/brain-structure-function/, Last accessed June, 2021.

[22] B. H. Menze et al., The Multimodal Brain Tumor Image Segmentation Benchmark (BRATS), in IEEE Transactions on Medical Imaging, vol. 34, no. 10, pp. 1993-2024, Oct. 2015, doi: 10.1109/TMI.2014.2377694

[23] Multimodal Segmentation of Brain Tumor Challenge 2020: Tasks. [online], https://www.med.upenn.edu/cbica/brats2020/tasks.html, Last accessed May, 2021

[24] Havaei, M., Davy, A., Warde-Farley, D., Biard, A., Courville, A., Bengio, Y., Pal, C., Jodoin, P.M. and Larochelle, H., 2017. Segmentation of Brain Tumor with deep neural networks. Medical image analysis, 35, pp.18-31

[25] S. Pereira, A. Pinto, V. Alves and C. A. Silva, Segmentation of Brain Tumor Using Convolutional Neural Networks in MRI Images, in IEEE Transactions on Medical Imaging, vol. 35, no. 5, pp. 1240-1251, May 2016, doi: 10.1109/TMI.2016.2538465

[26] Zhao, Xiaomei, Yihong Wu, Guidong Song, Zhenye Li, Yazhuo Zhang, and Yong Fan. A deep learning model integrating FCNNs and CRFs for Segmentation of Brain Tumor. Medical image analysis 43 (2018): 98-111

[27] Saouli, Rachida, Mohamed Akil, and Rostom Kachouri. Fully automatic Segmentation of Brain Tumor using end-to-end incremental deep neural networks in MRI images. Computer methods and programs in biomedicine 166 (2018): 39-49

[28] Zhao, Xiaomei, Yihong Wu, Guidong Song, Zhenye Li, Yazhuo Zhang, and Yong Fan. 3D Segmentation of Brain Tumor through integrating multiple 2D FCNNs. In International MICCAI Brainlesion Workshop, pp. 191-203. Springer, Cham, 2017

[29] Colmeiro, RG Rodríguez, C. A. Verrastro, and Thomas Grosges. Multimodal Segmentation of Brain Tumor using 3D convolutional networks. In International MICCAI Brainlesion Workshop, pp. 226-240. Springer, Cham, 2017

[30] Alex, Varghese, Mohammed Safwan, and Ganapathy Krishnamurthi. Automatic segmentation and overall survival prediction in gliomas using fully convolutional neural network and texture analysis. In International MICCAI Brainlesion Workshop, pp. 216-225. Springer, Cham, 2017.

[31] Soltaninejad, Mohammadreza, Lei Zhang, Tryphon Lambrou, Guang Yang, Nigel Allinson, and Xujiong Ye. MRI Segmentation of Brain Tumor and patient survival prediction using random forests and fully convolutional networks. In International MICCAI Brainlesion Workshop, pp. 204-215. Springer, Cham, 2017

[32] Li, Zeju, Yuanyuan Wang, Jinhua Yu, Zhifeng Shi, Yi Guo, Liang Chen, and Ying Mao. Low-grade glioma segmentation based on CNN with fully connected CRF. Journal of Healthcare Engineering 2017 (2017)

[33] Zhao, Xiaomei, Yihong Wu, Guidong Song, Zhenye Li, Yong Fan, and Yazhuo Zhang. Segmentation of Brain Tumor using a fully convolutional neural network with conditional random fields. In International Workshop on Brainlesion: Glioma, Multiple Sclerosis, Stroke and Traumatic Brain Injuries, pp. 75-87. Springer, Cham, 2016

[34] Chang, Peter D. Fully convolutional deep residual neural networks for Segmentation of Brain Tumor. In International Workshop on Brainlesion: Glioma, Multiple Sclerosis, Stroke and Traumatic Brain Injuries, pp. 108-118. Springer, Cham, 2016

[35] Myronenko, Andriy. 3D MRI Segmentation of Brain Tumor using autoencoder regularization. In International MICCAI Brainlesion Workshop, pp. 311-320. Springer, Cham, 2018.

[36] McKinley, Richard, Raphael Meier, and Roland Wiest. Ensembles of densely-connected CNNs with label-uncertainty for Segmentation of Brain Tumor. In International MICCAI Brainlesion Workshop, pp. 456-465. Springer, Cham, 2018

[37] Isensee, Fabian, Philipp Kickingereder, Wolfgang Wick, Martin Bendszus, and Klaus H. Maier-Hein. Segmentation of Brain Tumor and radiomics survival prediction: Contribution to the brats 2017 challenge. In International MICCAI Brainlesion Workshop, pp. 287-297. Springer, Cham, 2017

[38] Chen, Chen, Xiaopeng Liu, Meng Ding, Junfeng Zheng, and Jiangyun Li. 3D dilated multi-fiber network for real-time Segmentation of Brain Tumor in MRI. In International Conference on Medical Image Computing and Computer-Assisted Intervention, pp. 184-192. Springer, Cham, 2019

[39] Lachinov, Dmitry, Evgeny Vasiliev, and Vadim Turlapov. Glioma segmentation with cascaded UNet. In International MICCAI Brainlesion Workshop, pp. 189-198. Springer, Cham, 2018

[40] Li, Zeju, Yuanyuan Wang, and Jinhua Yu. Segmentation of Brain Tumor using an adversarial network. In International MICCAI Brainlesion Workshop, pp. 123-132. Springer, Cham, 2017

[41] Rezaei, Mina, Konstantin Harmuth, Willi Gierke, Thomas Kellermeier, Martin Fischer, Haojin Yang, and Christoph Meinel. A conditional adversarial network for semantic segmentation of brain tumor. In International MICCAI Brainlesion Workshop, pp. 241-252. Springer, Cham, 2017

[42] Xue, Yuan, Tao Xu, Han Zhang, L. Rodney Long, and Xiaolei Huang. Segan: Adversarial network with multi-scale l 1 loss for medical image segmentation. Neuroinformatics 16, no. 3-4 (2018): 383-392

[43] Domenico Cirillo, Marco, David Abramian, and Anders Eklund. Vox2Vox: 3D-GAN for Brain Tumour Segmentation. arXiv (2020): arXiv-2003

[44] Khosravanian, A., Rahmanimanesh, M., Keshavarzi, P. and Mozaffari, S., 2021. Fast level set method for glioma Segmentation of Brain Tumor based on Superpixel fuzzy clustering and lattice Boltzmann method. Computer Methods and Programs in Biomedicine, 198, p.105809

[45] Khan, A.R., Khan, S., Harouni, M., Abbasi, R., Iqbal, S. and Mehmood, Z., 2021. Segmentation of Brain Tumor using K-means clustering and deep learning with synthetic data augmentation for classification. Microscopy Research and Technique

[46] Chen, H., Qin, Z., Ding, Y., Tian, L. and Qin, Z., 2020. Segmentation of Brain Tumor with deep convolutional symmetric neural network. Neurocomputing, 392, pp.305-313

[47] Zhou, X., Li, X., Hu, K., Zhang, Y., Chen, Z. and Gao, X., 2021. ERV-Net: An efficient 3D residual neural network for Segmentation of Brain Tumor. Expert Systems with Applications, 170, p.114566

[48] Pei, L., Bakas, S., Vossough, A., Reza, S.M., Davatzikos, C. and Iftekharuddin, K.M., 2020. Longitudinal Segmentation of Brain Tumor prediction in MRI using feature and label fusion. Biomedical Signal Processing and Control, 55, p.101648

[49] Naser, M.A. and Deen, M.J., 2020. Segmentation of Brain Tumor and grading of lower-grade glioma using deep learning in MRI images. Computers in biology and medicine, 121, p.103758

[50] Zeineldin, R.A., Karar, M.E., Coburger, J., Wirtz, C.R. and Burgert, O., 2020. DeepSeg: deep neural network framework for automatic Segmentation of Brain Tumor using magnetic resonance FLAIR images. International journal of computer assisted radiology and surgery, 15(6), pp.909-920

[51] Zeineldin, R.A., Karar, M.E., Coburger, J. et al. DeepSeg: deep neural network framework for automatic brain tumor segmentation using magnetic resonance FLAIR images. Int J CARS 15, 909–920 (2020). https://doi.org/10.1007/s11548-020-02186-z

[52] Pei, L., Vidyaratne, L., Rahman, M.M. et al. Context aware deep learning for brain tumor segmentation, subtype classification, and survival prediction using radiology images. Sci Rep 10, 19726 (2020). https://doi.org/10.1038/s41598-020-74419-9

[53] Ghosh, S., Chaki, A. Santosh, K. Improved U-Net architecture with VGG-16 for brain tumor segmentation. Phys Eng Sci Med (2021). https://doi.org/10.1007/s13246-021-01019-w

[54] Alqazzaz, S., Sun, X., Yang, X. et al. Automated brain tumor segmentation on multi-modal MR image using SegNet. Comp. Visual Media 5, 209–219 (2019). https://doi.org/10.1007/s41095-019-0139-y

[55] Kaewrak K., Soraghan J., Di Caterina G., Grose D. (2021) TwoPath U-Net for Automatic Brain Tumor Segmentation from Multimodal MRI Data. In: Crimi A., Bakas S. (eds) Brainlesion: Glioma, Multiple Sclerosis, Stroke and Traumatic Brain Injuries. BrainLes 2020. Lecture Notes in Computer Science, vol 12659. Springer, Cham. https://doi.org/10.1007/978-3-030-72087-2-26

[56] Agravat, R. and Raval, M.S., 2020. 3D Semantic Segmentation of Brain Tumor for Overall Survival Prediction. arXiv preprint arXiv:2008.11576

[57] Anand, V.K., Grampurohit, S., Aurangabadkar, P., Kori, A., Khened, M., Bhat, R.S. and Krishnamurthi, G., 2021. Segmentation of Brain Tumor and Survival Prediction using Automatic Hard mining in 3D CNN Architecture. arXiv preprint arXiv:2101.01546

[58] Kao, P.Y., Ngo, T., Zhang, A., Chen, J.W. and Manjunath, B.S., 2018, September. Segmentation of Brain Tumor and tractographic feature extraction from structural MR images for overall survival prediction. In International MICCAI Brainlesion Workshop (pp. 128-141). Springer, Cham

[59] Puybareau, E., Tochon, G., Chazalon, J. and Fabrizio, J., 2018, September. Segmentation of gliomas and prediction of patient overall survival: a simple and fast procedure. In International MICCAI Brainlesion Workshop (pp. 199-209). Springer, Cham

[60] Shboul, Z.A., Vidyaratne, L., Alam, M. and Iftekharuddin, K.M., 2017, September. Glioblastoma and survival prediction. In International MICCAI Brainlesion Workshop (pp. 358-368). Springer, Cham

[61] Feng, X., Tustison, N.J., Patel, S.H. and Meyer, C.H., 2020.. Frontiers in Segmentation of Brain Tumor using an ensemble of 3d u-nets and overall survival prediction using radiomic features computational neuroscience, 14, p.25

[62] Zhao G., Jiang B., Zhang J., Xia Y. (2021) Segmentation then Prediction: A Multi-task Solution to Segmentation of Brain Tumor and Survival Prediction. In: Crimi A., Bakas S. (eds) Brainlesion: Glioma, Multiple Sclerosis, Stroke and Traumatic Brain Injuries. BrainLes 2020. Lecture Notes in Computer Science, vol 12658. Springer, Cham

[63] Ali M.J., Akram M.T., Saleem H., Raza B., Shahid A.R. (2021) Glioma Segmentation Using Ensemble of 2D/3D U-Nets and Survival Prediction Using Multiple Features Fusion. In: Crimi A., Bakas S. (eds) Brainlesion: Glioma, Multiple Sclerosis, Stroke and Traumatic Brain Injuries. BrainLes 2020. Lecture Notes in Computer Science, vol 12659. Springer, Cham. https://doi.org/10.1007/978-3-030-72087-2_17

[64] Mitchell, Tom M. "Machine learning." (1997).

[65] Uddin, Shahadat, Arif Khan, Md Ekramul Hossain, and Mohammad Ali Moni. "Comparing different supervised machine learning algorithms for disease prediction." BMC medical informatics and decision making 19, no. 1 (2019): 1-16.

[66] Shailaja, K., B. Seetharamulu, and M. A. Jabbar. "Machine learning in healthcare: A review." In 2018 Second international conference on electronics, communication and aerospace technology (ICECA), pp. 910-914. IEEE, 2018.

[67] Emami, Melikasadat, Mojtaba Sahraee-Ardakan, Parthe Pandit, Sundeep Rangan, and Alyson Fletcher. "Generalization error of generalized linear models in high dimensions." In International Conference on Machine Learning, pp. 2892-2901. PMLR, 2020.

[68] Bengio, Yoshua, Ian Goodfellow, and Aaron Courville. Deep learning. Vol. 1. Massachusetts, USA:: MIT press, 2017.

[69] Brownlee, Jason. Master Machine Learning Algorithms: discover how they work and implement them from scratch. Machine Learning Mastery, 2016.

[70] Morid, Mohammad Amin, Kensaku Kawamoto, Travis Ault, Josette Dorius, and Samir Abdelrahman. Supervised learning methods for predicting healthcare costs: systematic literature review and empirical evaluation. In AMIA Annual Symposium Proceedings, vol. 2017, p. 1312. American Medical Informatics Association, 2017.

[71] Christodoulou, Evangelia, Jie Ma, Gary S. Collins, Ewout W. Steyerberg, Jan Y. Verbakel, and Ben Van Calster. A systematic review shows no performance benefit of machine learning over logistic regression for clinical prediction models. Journal of clinical epidemiology 110 (2019): 12-22.

[72] Takahashi, Yuta, Masao Ueki, Makoto Yamada, Gen Tamiya, Ikuko N. Motoike, Daisuke Saigusa, Miyuki Sakurai et al. Improved metabolomic data-based prediction of depressive symptoms using nonlinear machine learning with feature selection. Translational psychiatry 10, no. 1 (2020): 1-12.

[73] J. Friedman, T. Hastie, R. Tibshirani, The elements of statistical learning, volume 1, Springer series in statistics New York, 2001.

[74] G. James, D. Witten, T. Hastie, R. Tibshirani, An introduction to statistical learning, volume 112, Springer, 2013.

[75] Bianchini, M. and Scarselli, F., 2014. On the complexity of neural network classifiers: A comparison between shallow and deep architectures. IEEE transactions on neural networks and learning systems, 25(8), pp.1553-1565.

[76] Neural Networks and Deep Learning. [online], http://neuralnetworksanddeeplearning.com/, Last accessed June, 2021.

[77] Reynolds Blogs. [online], https://anhreynolds.com/blogs/cnn.html, Last accessed June, 2021.

[78] Numpy Ninja. [online], https://www.numpyninja.com/post/how-padding-helps-in-cnn, Last accessed June, 2021

[79] Blog. [online], http://makeyourownneuralnetwork.blogspot.com/2020/02/calculating-output-size-of-convolutions.html, Last accessed June, 2021

[80] Github. [online], https://mohameddhaoui.github.io/deeplearning/CNN_tuto2/], Last accessed June, 2021

[81] Soriano, Danny, Carlos Aguilar, Ivan Ramirez-Morales, Eduardo Tusa, Wilmer Rivas, and Maritza Pinta. Mammogram classification schemes by using convolutional neural networks.In International Conference on Technology Trends, pp. 71-85. Springer, Cham, 2017.

[82] Blog. [online], https://hmkcode.com/ai/backpropagation-step-by-step/], Last accessed June, 2021

[83] Krizhevsky, Alex, Ilya Sutskever, and Geoffrey E. Hinton. "Imagenet classification with deep convolutional neural networks." Advances in neural information processing systems 25 (2012): 1097-1105.

[84] Data Science Central. [online], https://www.datasciencecentral.com/profiles/blogs/alexnet-implementation-using-keras, Last accessed June, 2021

[85] Ronneberger, Olaf, Philipp Fischer, and Thomas Brox. "U-net: Convolutional networks for biomedical image segmentation." In International Conference on Medical image computing and computer-assisted intervention, pp. 234-241. Springer, Cham, 2015.

[86] Simonyan, Karen, and Andrew Zisserman. "Very deep convolutional networks for large-scale image recognition." arXiv preprint arXiv:1409.1556 (2014).

[87] Menze, Bjoern H., Andras Jakab, Stefan Bauer, Jayashree Kalpathy-Cramer, Keyvan Farahani, Justin Kirby, Yuliya Burren et al. "The multimodal brain tumor image segmentation benchmark (BRATS)." IEEE transactions on medical imaging 34, no. 10 (2014): 1993-2024.

[88] Jain, S., Shukla, S. and Wadhvani, R., 2018. Dynamic selection of normalization techniques using data complexity measures. Expert Systems with Applications, 106, pp.252-262.

[89] Brunese, Luca, Francesco Mercaldo, Alfonso Reginelli, and Antonella Santone. "An ensemble learning approach for brain cancer detection exploiting radiomic features." Computer methods and programs in biomedicine 185 (2020): 105134.

[90] Hossin, M. and Sulaiman, M.N., 2015. A review on evaluation metrics for data classification evaluations. International Journal of Data Mining Knowledge Management Process, 5(2), p.1.

[91] Ghaffari, Mina, Arcot Sowmya, and Ruth Oliver. "Brain tumour segmentation using cascaded 3D densely-connected U-net." arXiv preprint arXiv:2009.07563 (2020).

[92] Ballestar, Laura Mora, and Veronica Vilaplana. "Segmentation of Brain Tumor using 3D-CNNs with Uncertainty Estimation." arXiv preprint arXiv:2009.12188 (2020).

[93] Colman, Jordan, Lei Zhang, Wenting Duan, and Xujiong Ye. "DR-Unet104 for Multimodal MRI Segmentation of Brain Tumor." arXiv preprint arXiv:2011.02840 (2020).

[94] Silva C.A., Pinto A., Pereira S., Lopes A. (2021) Multi-stage Deep Layer Aggregation for Brain Tumor Segmentation. In: Crimi A., Bakas S. (eds) Brainlesion: Glioma, Multiple Sclerosis, Stroke and Traumatic Brain Injuries. BrainLes 2020. Lecture Notes in Computer Science, vol 12659. Springer, Cham. https://doi.org/10.1007/978-3-030-72087-216

[95] Murugesan G.K. et al. (2021) Multidimensional and Multiresolution Ensemble Networks for Brain Tumor Segmentation. In: Crimi A., Bakas S. (eds) Brain-

lesion: Glioma, Multiple Sclerosis, Stroke and Traumatic Brain Injuries. Brain-Les 2020. Lecture Notes in Computer Science, vol 12658. Springer, Cham. https://doi.org/10.1007/978-3-030-72084-140

[96] Qamar S., Ahmad P., Shen L. (2021) HI-Net: Hyperdense Inception 3D UNet for Brain Tumor Segmentation. In: Crimi A., Bakas S. (eds) Brainlesion: Glioma, Multiple Sclerosis, Stroke and Traumatic Brain Injuries. BrainLes 2020. Lecture Notes in Computer Science, vol 12659. Springer, Cham. https://doi.org/10.1007/978-3-030-72087-25

[97] Cui, Shaoguo, Lei Mao, Jingfeng Jiang, Chang Liu, and Shuyu Xiong. "Automatic semantic segmentation of brain gliomas from MRI images using a deep cascaded neural network." Journal of healthcare engineering 2018 (2018).

[98] Hoseini, Farnaz, Asadollah Shahbahrami, and Peyman Bayat. "An efficient implementation of deep convolutional neural networks for MRI segmentation." Journal of digital imaging 31, no. 5 (2018): 738-747

[99] Kamnitsas, Konstantinos, Wenjia Bai, Enzo Ferrante, Steven McDonagh, Matthew Sinclair, Nick Pawlowski, Martin Rajchl et al. "Ensembles of multiple models and architectures for robust brain tumour segmentation." In International MICCAI brain-lesion workshop, pp. 450-462. Springer, Cham, 2017